

**DEVELOPMENT OF ULTRASENSITIVE
VOLTAMMETRIC ION-SELECTIVE ELECTRODES**

by

Mohammed Basem Garada

B.A. in Chemistry, Boston University, 2012

Submitted to the Graduate Faculty of
the Dietrich School of Arts and Sciences in partial fulfillment
of the requirements for the degree of
Master of Science in Chemistry

University of Pittsburgh

2015

UNIVERSITY OF PITTSBURGH
Dietrich School of Arts and Sciences

This thesis was presented

by

Mohammed Basem Garada

It was defended on

November 21, 2014

and approved by

Adrian Michael, Professor, Department of Chemistry

Stephen Weber, Professor, Department of Chemistry

Committee Chair: Shigeru Amemiya, Associate Professor, Department of Chemistry

Copyright © by Mohammed Basem Garada

2015

**DEVELOPMENT OF ULTRASENSITIVE
VOLTAMMETRIC ION-SELECTIVE ELECTRODES**

Mohammed Basem Garada, M.S.

University of Pittsburgh, 2015

Low concentration detection of ions is an important part of many industrial and medical fields. While current technologies in the form of ion chromatography and LC/MS present a reliable means of sensitive ion detection, they also can be quite expensive and bulky, and thus not always readily available to those who need them. Ion-selective electrodes offer a good alternative in the form of cheaper and smaller tools for ion detection. Most importantly, the level of detection of ion-selective electrodes can match that of more expensive methods and in some cases go beyond them. Through ion-transfer voltammetry ultrasensitive electrodes are created and used to be able to detect ions at sub-nanomolar levels. The specific electrodes used here consist of a gold electrode coated by an ion-to-electron transducing conducting polymer further overlain with an ionophore-doped organic PVC membrane. Various types of ions have been studied by both cyclic voltammetry and stripping voltammetry, including hydrophilic inorganic ions (Ca^{2+}), hydrophobic organic surfactants (PFOS^-) and biologically relevant macromolecules (protamine²⁰⁺). Detection of surfactants is highlighted here, with an emphasis on an achievable detection limit of 50pM for PFOS^- without any ionophore. This detection limit which is in fact lower than the EPA minimum reporting level was made possible due to the very high lipophilicity of PFOS^- which allows it to be concentrated into the organic PVC layer to a greater extent during ion-transfer stripping voltammetry. Other surfactants including alkyl carboxylates, alkyl sulfonates and perfluorinated

carboxylates were also tested, but a focus was made on PFOS⁻ due to it being the most lipophilic on the EPA's list of environmentally important surfactants. It was found that the conducting polymer used for surfactant detection, POT, led to oxidation of certain carboxylate surfactants. Previous issues of reduction of certain cations like Ag⁺ and Pb²⁺ with the other conducting polymer used, PEDOT, as well as lack of a stable potential for both POT and PEDOT led us to synthesize and electrochemically polymerize a new conducting polymer, 4,4'-dibutoxy-2,2'-bithiophene. This marks the first such electrochemical polymerization of this dimer.

TABLE OF CONTENTS

PREFACE	xi
1.0 INTRODUCTION	1
2.0 PICOMOLAR PFOS⁻ DETECTION AND SURFACTANT LIPOPHILICITY	4
2.1 INTRODUCTION	4
2.2 EXPERIMENTAL	8
2.2.1 Chemicals	8
2.2.2 Electrode Modification	9
2.2.3 Electrochemical Measurement	10
2.3 RESULTS AND DISCUSSION	11
2.3.1 Cyclic Voltammetry of Perfluoroalkanesulfonates	11
2.3.2 Lipophilicity of Perfluoroalkanesulfonates: Fragmental Analysis	15
2.3.3 Lipophilicity and Fluorophilicity of Perfluoroalkanesulfonates	17
2.3.4 Stripping Voltammetry of PFOS⁻	18
2.3.5 Picomolar Detection Limit for PFOS⁻	22
2.3.6 Cyclic Voltammetry of Perfluoroalkancarboxylates	25
2.3.7 Voltammetry versus Potentiometry with the oNPOE/PVC Membrane	29
2.4 CONCLUSIONS	30
2.5 SUPPORTING INFO	31
2.5.1 Cyclic Voltammetry of Alkyl Sulfonates	31
2.5.2 Background-Subtracted Stripping Voltammograms of Picomolar PFOS⁻	33
2.5.3 Stripping Voltammetric Responses to a Contaminant Anion	35
2.5.4 Lipophilicity of Perfluoroalkyl Carboxylates	37
2.5.5 Oxidation of PFO⁻ at the PVC/POT/Gold Junction	39
3.0 DEVELOPMENT OF NEW CONDUCTING POLYMER: POLY(4,4'-DIBUTOXY-2,2'-BITHIOPHENE)	41
3.1 BACKGROUND	41
3.2 SYNTHESIS OF 4,4'-DIBUTOXY-2,2'-BITHIOPHENE	42
3.3 ELECTROCHEMICAL POLYMERIZATION	46
4.0 CONCLUSIONS	50
BIBLIOGRAPHY	51

LIST OF FIGURES

- Figure 1.** Scheme of the voltammetric transfer of PFOS^- from water into the oNPOE/PVC membrane coated on a POT-modified Au electrode at positive potentials. Charge transfer between the POT film and the oNPOE/PVC membrane is mediated by organic electrolytes in the membrane..... 7
- Figure 2.** Background-subtracted CVs (red lines) of 20 μM perfluorooctanesulfonate, perfluorohexanesulfonate, perfluorobutanesulfonate, and octanesulfonate (from the top) in cell 1. The potential was applied to the gold electrode, swept at 0.1 V/s, and defined against the formal potential of perchlorate. Circles represent the CVs simulated by using the parameters listed in Table S-1 (Supporting Information). Dotted lines correspond to the formal potentials of the sulfonates. 13
- Figure 3.** Formal potentials versus the number of carbon atoms of perfluoroalkanesulfonates (closed circles) and alkanesulfonates (crosses) for the oNPOE/PVC membrane. The formal potentials of the perfluoroalkanesulfonates for the fluorous membrane (open circles) were calculated from selectivity coefficients against perchlorate³⁶ by using eq. 4. Solid lines are the best fits with eq. 3..... 16

Figure 4. (A) Stripping voltammograms of 10 nM PFOS⁻ (cell 2) at different preconcentration times. The potential was applied to the gold electrode, swept at 0.1 V/s, and defined against the formal potential of perchlorate. (B) Charge during stripping voltammetry (circles) and best fit with eq. 6 (solid line). 21

Figure 5. (A) Stripping voltammograms of 0–1 nM PFOS⁻ (cell 2) after 30 min of preconcentration. The potential was applied to the gold electrode, swept at 0.1 V/s, and defined against the formal potential of perchlorate. (B) Background-subtracted peak current versus PFOS⁻ concentration (circles) and best fit with eq. 9 (solid line)..... 24

Figure 6. Background-subtracted CVs (red lines) of 20 μM perfluorooctanoate, perfluorohexanoate, and perfluorobutanoate and 10 μM tetradecanoate (from the top) in cell 1. The potential was applied to the gold electrode, swept at 0.1 V/s, and defined against the formal potential of perchlorate. Circles represent the CVs simulated by using the parameters listed in Table S-1 (Supporting Information). Dotted lines correspond to the formal potentials of the sulfonates with the same number of carbon atoms. 27

Figure 7. Background-subtracted CVs (red lines) of 20 μM dodecyl and decyl sulfonates (from the top) in cell 1. The potential was applied to the gold electrode, swept at 0.1 V/s, and defined against the formal potential of perchlorate. Dotted lines correspond to the formal potentials of the sulfonates. 32

Figure 8. Background-subtracted stripping voltammograms of 0.05–1 nM PFOS⁻ (cell 2) after 30 min preconcentration. The potential was applied to the gold electrode, swept at 0.1 V/s, and defined against the formal potential of perchlorate. The dotted line represents zero current..... 34

Figure 9. Stripping voltammograms of 0–1 nM PFOS⁻ (cell 2) after 30 min preconcentration in the presence of a contaminant anion in the sample solutions. The potential was applied to the gold electrode, swept at 0.1 V/s, and defined against the formal potential of perchlorate. 36

Figure 10. Background-subtracted CVs (red lines) of 20 μM perfluorododecanoate and perfluorodecanoate (from the top) in cell 1. The potential was applied to the gold electrode, swept at 0.1V/s, and defined against the formal potential of perchlorate. The dotted line corresponds to the formal potential of PFOS⁻ 38

Figure 11. CVs of a POT film with a PVC membrane/water interface non-polarized by partitioning of TBAClO₄. The potential was applied to the gold electrode against a Ag/AgCl reference electrode in 3 M KCl. Potential sweep rate, 0.1 V/s..... 40

Figure 12. Proposed new conducting polymer in its dimer form: 4,4'-dibutoxy-2,2'-bithiophene 41

Figure 13. Synthesis of 4,4'-dibutoxy-2,2'-bithiophene from 4,4'-dibromo-2,2'-bithiophene... 42

Figure 14. Hypothesized step-wise halogen exchange and butoxylation of 4,4'-dibromo-2,2'-bithiophene leading to the monobutoxy side product 4-bromo-4'-butoxy-2,2'-bithiophene 43

Figure 15. Electropolymerization of 4,4'-bitoxy-2,2'-bithiophene in acetonitrile (C = 0.01M) with TDDA-TFAB (C = 0.03M); Scan rate = 0.1V/s, Au working electrode, Pt wire reference electrode, carbon graphite cell as counter electrode. The potential was cycled three times and ended at the negative side of the potential window. 47

Figure 16. Monomer free CV of poly(4,4'-bitoxy-2,2'-bithiophene) in acetonitrile with TDDA-TFAB (C = 0.03M); Scan rate = 0.1V/s, Au working electrode, Pt wire reference electrode, carbon graphite cell as counter electrode. The potential was cycled three times starting at the negative side of the potential window and ending at the positive side. 48

PREFACE

I would like to thank my advisor Dr. Amemiya for his mentoring and support, and for him giving me the opportunity to perform research in his group. I also would like to thank Benjamin Kabagambe for his guidance as well as the other members of the Amemiya group for their help and companionship. Lastly I want to thank my committee members Dr. Michael and Dr. Weber for their time and consideration as well as the Department of Chemistry and the University of Pittsburgh as a whole for their support.

1.0 INTRODUCTION

Through this research we aim to develop and demonstrate the application of voltammetric ion-selective electrodes of unsurpassed sensitivity (sub-nanomolar detection limits) towards ions of environmental and biological importance.

Ion-transfer voltammetric methods have proven as useful tools in studying important ions such as K^+ , NH_4^+ , Ag^+ , Ca^{2+} , Ba^{2+} and Pb^{2+} without their electrolysis.^{1,2,3} Of particular importance is the use of ion-transfer stripping voltammetry (ITSV) as an inexpensive and faster alternative to traditionally more powerful trace analysis methods (e.g. LC-MS).¹ Indeed, the detection limits of ions studied by ITSV can be lowered to similar or even lower levels than the limits obtained from highly sensitive analytical methods.⁴ Lower detection limits are critical in both medical and environmental applications where the close monitoring of ions such as biological electrolytes, charged macromolecules, water contaminants and toxic agents is essential.⁵

Developments in ion-transfer voltammetry in our laboratory have led to the use of double-polymer-modified electrodes, which consist of a plasticized poly(vinyl chloride) (PVC) membrane as an ion-selective phase and a redox capable conducting polymer as an ion-to-electron transducing layer.^{4,6,7} Two such prominent polymers include poly(3-octylthiophene) (POT) and poly(3,4-ethylenedioxythiophene) (PEDOT).^{8,9,10} Depending on the type of ion being studied (cation vs. anion), the correct conducting polymer can be used, and specifically the correct oxidation state of the polymer.⁴ For instance, in its ion-transfer voltammetric application, the oxidized form of

PEDOT is reduced by a negative potential which conjunctly allows the transfer of a cation from the water phase into the plasticized PVC membrane.¹ Conversely, for the transfer of anions from the water phase into the PVC membrane the neutral form of POT can be used and subsequently oxidized by a positive potential to aid in the ion transfer.⁶ Some limitations of these conducting polymers manifest in the form of irreproducible redox potentials, short lifetimes for certain oxidation states, and unwanted redox reactions of the sample ions themselves.¹¹

In order to aid in the transfer of hydrophilic ions from the water phase into the hydrophobic PVC membrane, certain ionophores which exhibit selective binding to the ion of interest can be incorporated directly into the PVC membrane.^{1,2,3} The strength of the ion-ionophore interaction can be tuned via careful structural modification of the ionophore, overall resulting in enhanced ion sensitivity.² Furthermore, ion selectivity is also increased through more specific ion-ionophore interactions, which is necessary to avoid unwanted current responses from interfering ions.²

ITSV involves the accumulation of aqueous ions into an organic phase and then the subsequent “stripping” of these ions back into the aqueous phase. The key feature and usefulness of ITSV is that a relatively large amount of ions can be preconcentrated from very minimal concentrations (nanomolar and subnanomolar levels) thereby resulting in a significant current response upon the stripping step.⁴ Directly related to the amount of sample preconcentrated into the membrane is the potential applied to the electrode during preconcentration (preconcentration potential). More negative preconcentration potentials result in increased preconcentration of cations, while more positive preconcentration potentials cause the same for anions. While it is important to have a large preconcentration potential in order to maximize ion accumulation, an important limitation is the transfer of the aqueous background supporting electrolytes if too extreme potentials are used.

Another fundamental feature of ITSV is the length of time spent preconcentrating (preconcentration time), in that the amount of ions accumulated into the organic phase is directly proportional to preconcentration time.¹¹ In order to maximize the stripping current response and hence achieve the lowest detection limit, longer preconcentration times on the scale of around 30 minutes are typically used, in contrast to shorter times (≤ 5 minutes). Here, a limitation is on the capacity of the organic phase for the ion in question, whereby excessively long preconcentration times will result in saturation of the PVC membrane and thus a stripping current response that no longer grows beyond a certain current level.¹² Beyond tunable features of ITSV, inherent features of the ions being studied including ion charge number¹² and lipophilicity¹¹ can directly influence the possible stripping peak current response. In detail, the peak current response will be proportional to the given ion's charge number, while more lipophilic ions are capable of being more easily accumulated into the hydrophobic PVC membrane allowing for a higher preconcentration potential to be applied.

Cyclic voltammetry (CV) measurements are less suited for ultrasensitive detection and are more practical for quick elucidation of information of the ion being studied such as bulk concentration (as low as micromolar or submicromolar levels), kinetic behavior (can be compared directly to theoretical values through simulation), adsorption behavior (based on accumulated charge through CV integration) and ion lipophilicity (through standard potential trends among different ions).^{11, 12}

2.0 PICOMOLAR PFOS⁻ DETECTION AND SURFACTANT LIPOPHILICITY

This work is available as:

Garada, M. B., Kabagambe, B., Kim, Y., and Amemiya, S., Ion-Transfer Voltammetry of Perfluoroalkanesulfonates and Perfluoroalkancarboxylates: Picomolar Detection Limit and High Lipophilicity. *Anal. Chem.* **2014**, 86 (22), 11230–11237.

2.1 INTRODUCTION

Significant attention has been given to the electrochemical studies of perfluoroalkanesulfonates and perfluoroalkancarboxylates, which need to be monitored¹³ and remediated¹⁴ owing to environmental persistence¹⁵ and public health effects.¹⁶ The oxidation of these perfluoroalkyl oxoanions has been demonstrated for remediation by generating hydroxyl radicals at the electrodes based on boron-doped diamond,^{17, 18, 19, 20} SnO₂,²¹ and PbO₂.²² By contrast, the perfluoroalkyl oxoanions are less amenable to direct electrode reactions than their nonfluorinated analogues,¹⁴ thereby hampering electrochemical detection. The oxidation of the anionic head groups is slowed by the inductive effect of perfluorination on their electron density, thereby limiting the Kolbe-type decarboxylation of perfluoroalkancarboxylates.²³ Oxidative defluorination is even more difficult because of the high electronegativity of fluorine atoms. Reductive defluorination is also sluggish at platinum and carbon electrodes.²⁴ Alternatively, an electrochemical biosensor based on the

inhibition of glutamic dehydrogenase by perfluorooctanesulfonate (PFOS⁻) was developed to achieve a low detection limit of 1.6 nM, i.e., 0.80 µg/L.²⁵ The U.S. Environmental Protection Agency (EPA), however, set much lower concentrations as the minimum reporting levels for the assessment monitoring of PFOS⁻ (0.04 µg/L), perfluorooctanoate (PFO⁻; 0.02 µg/L), and four homologous compounds (0.01–0.09 µg/L) in drinking water.²⁶ Presently, this challenging analytical task requires LC/MS/MS coupled with solid-phase extraction.²⁷

Recently, we applied ion-transfer micropipet voltammetry^{28, 29} at the interface between 1-octanol and water to find that perfluoroalkyl oxoanions are ~102 times more lipophilic than their alkyl counterparts.³⁰ Significantly, this finding supports the hypothesis that the bioaccumulation and toxicity of the perfluoroalkyl oxoanions originate from their lipophilic nature.³¹ The higher lipophilicity of the perfluoroalkyl oxoanions is due to the strong electron-withdrawing effect of the perfluoroalkyl group on the adjacent oxoanion group, which is weakly hydrated to decrease its hydrophilicity. By contrast, perfluoroalkyl and alkyl chains with the same length are similarly hydrophobic. These conclusions were made separately by conducting the fragmental analysis³² of the formal partition coefficient, $P_i^{0'}$, of a target ion, i , as a measure of ion lipophilicity. The formal partition coefficient was determined from the formal potential, $\Delta_w \phi_i^{0'}$, as given by³³

$$\log P_i^{0'} = \frac{z_i F \Delta_w \phi_i^{0'}}{2.303RT} \quad (1)$$

where z_i is the charge of the target ion. Experimentally, the formal potential as well as all kinetic and mass-transport parameters were obtainable³⁴ by ion-transfer cyclic voltammetry at micropipet-supported 1-octanol/water interfaces. The thermodynamically favorable and fast transfer of the perfluoroalkyl oxoanions is advantageous for their selective electrochemical detection without the need for their electrolysis. However, neither a fragile micropipet electrode nor fluidic 1-octanol is suitable for practical sensing applications.

In this work, we take advantage of the high lipophilicity of perfluoroalkyl oxoanions to enable ion-transfer voltammetric detection at a picomolar level. Importantly, ion-transfer stripping voltammetry with a thin double-polymer membrane coated on a solid electrode³⁵ (Figure 1) gives a lower detection limit for a more lipophilic ion.⁷ We characterize the lipophilicity of a homologous series of PFOS⁻ and PFO⁻ voltammetrically by employing a ~1 μm thick poly(vinyl chloride) (PVC) membrane plasticized with 2-nitrophenyl octyl ether (oNPOE) as a robust ion-selective membrane. In contrast to our recent studies of hydrophilic potassium¹ and calcium¹² ions, no ionophore is needed to transfer the lipophilic anions into the lipophilic membrane. The oNPOE/PVC membrane is supported by a gold electrode modified with a poly(3-octylthiophene) (POT) film as a voltammetric ion-to-electron transducer.^{4,6}

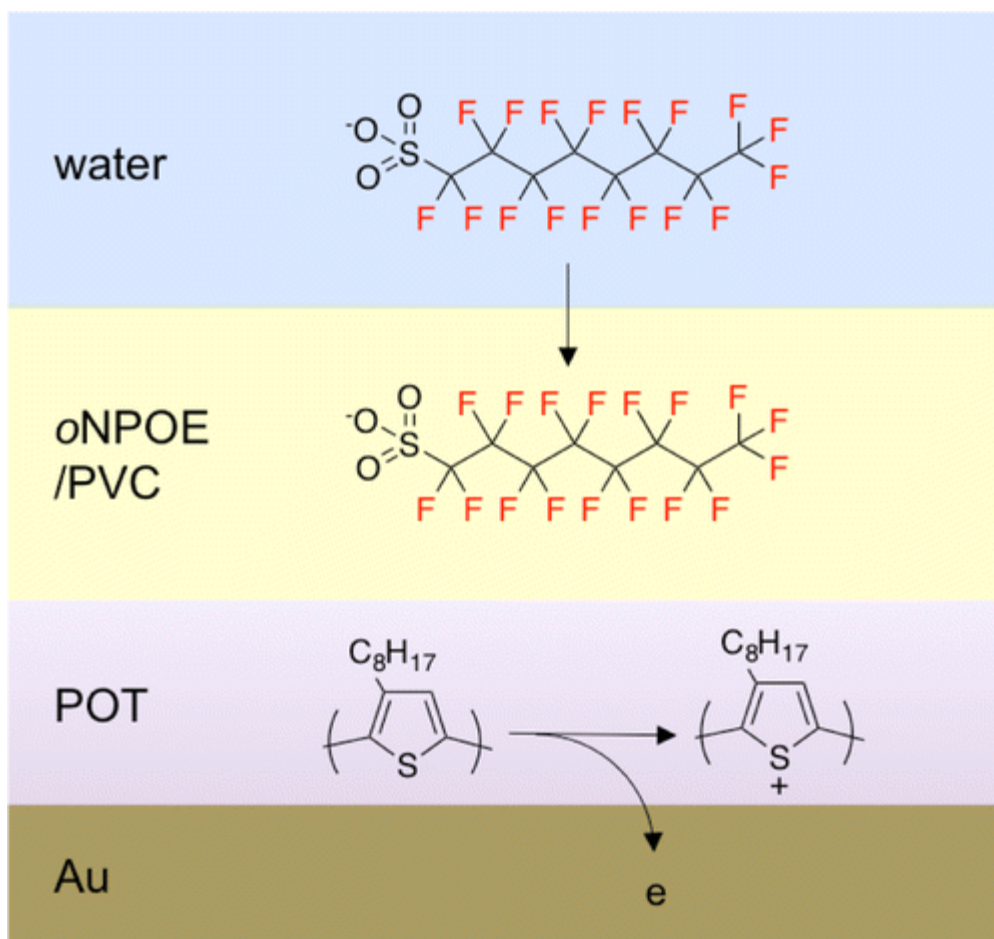


Figure 1. Scheme of the voltammetric transfer of PFOS⁻ from water into the oNPOE/PVC membrane coated on a POT-modified Au electrode at positive potentials. Charge transfer between the POT film and the oNPOE/PVC membrane is mediated by organic electrolytes in the membrane.

Specifically, we demonstrate that PFOS⁻ is the most lipophilic among the six perfluoroalkyl oxoanions monitored by the U.S. EPA²⁶ and is detectable by ion-transfer stripping voltammetry at a remarkably low concentration of 50 pM (0.025 µg/L) in the presence of 1 mM aqueous supporting electrolytes, i.e., a 7 orders of magnitude higher concentration. Significantly, this detection limit is below the minimum reporting level of PFOS⁻ set by the U.S. EPA²⁶ and is lower than that achieved by any electrochemical sensor for perfluoroalkyl oxoanions, including potentiometry with a fluorous membrane, i.e., 0.86 nM PFOS⁻ and 0.17 nM PFO⁻.³⁶ In comparison, perfluoroalkylcarboxylates are less lipophilic and more oxidizable at the POT-modified gold electrode, which not only compromises their voltammetric detection but also manifests the limitation of the POT film as a voltammetric ion-to-electron transducer. In addition, we reveal that the fluorophilicity of perfluoroalkyl oxoanions^{36,37} is higher than their lipophilicity, which renders the fluorous membrane attractive for ultrasensitive ion-transfer voltammetry of the multiple perfluoroalkyl oxoanions monitored by the U.S. EPA.

2.2 EXPERIMENTAL

2.2.1 Chemicals

The sodium salt of PFO⁻ was obtained from Strem Chemicals (Newburyport, MA). The potassium salt of PFOS⁻ was obtained from Synquest Laboratories (Alachua, FL). The potassium salts of the other perfluoroalkanesulfonates, the sodium salts of alkanesulfonates, the perfluoroalkylcarboxylic acids, tetradodecylammonium (TDDA) bromide, PVC (high molecular weight), oNPOE (≥99.0%), 3-octylthiophene, potassium chloride (≥99.9995%), Li₂SO₄ (≥99.99%), and LiClO₄ were purchased from Aldrich (Milwaukee, WI). The

perfluoroalkancarboxylic acids were dissolved in a sample solution and converted to sodium forms by adding a solution of sodium hydroxide. Sodium tetradecanoate was obtained from TCI America (Portland, OR). Potassium tetrakis(pentafluorophenyl)borate (TFAB; Boulder Scientific Co., Mead, CO) was used to prepare TDDATFAB as the organic supporting electrolyte.⁶ All reagents were used as received.

All sample solutions were prepared by using water (18.2 M Ω ·cm and total organic carbon (TOC) of 3 ppb) from the Milli-Q Advantage A10 system equipped with Q-Gard T2 Pak and a Quantum TIX or TEX cartridge (EMD Millipore Corp., Billerica, MA).¹² The sample solutions were prepared by using polypropylene volumetric flasks (VITLAB GmbH, Grossostheim, Germany) and poured into polypropylene beakers (VITLAB GmbH) for electrochemical measurement. We used polypropylene flasks and beakers, which PFOS⁻ and PFO⁻ do not adsorb to in contrast to glass.³⁶ To prevent airborne contamination during storage, the flasks were filled with Milli-Q water and the beakers were immersed in Milli-Q water filled in polypropylene wide-mouth jars (Thermo Scientific, Marietta, OH).

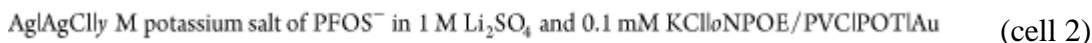
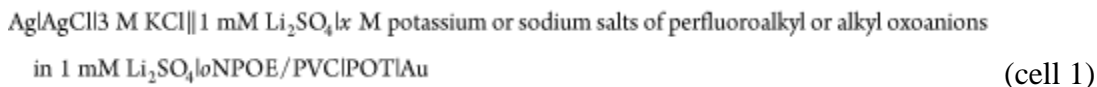
2.2.2 Electrode Modification

A 5 mm diameter gold disk attached to a rotating disk electrode tip (Pine Research Instrumentation, Raleigh, NC) was modified with a POT film and then with an oNPOE/PVC membrane (Figure 1) as follows. To minimize airborne contamination, a bare gold disk was cleaned as reported elsewhere.¹² A POT film was electrochemically deposited onto the gold disk from an acetonitrile solution containing 0.1 M 3-octylthiophene and 0.03 M TDDATFAB by using a 13 mm diameter graphite rod (99%, Alfa Aesar, Ward Hill, MA) as the counter electrode and a POT-modified Pt

wire as the quasi-reference electrode.³⁸ The potential of the gold electrode was controlled by using an electrochemical workstation (CHI 600A, CH Instruments, Austin, TX) and cycled four times at 0.1 V/s between -0.50 V and the switching potentials that yield a current of 0.65 mA for monomer oxidation. The final potential was set to -0.50 V to obtain a neutral POT film in the reduced form. The POT-modified gold electrode was soaked in acetonitrile for 30 min and then in THF for 1 min to remove the soluble fractions of the POT film. Then an oNPOE/PVC membrane was spin-coated onto the POT-modified gold electrode from a solution containing 4 mg of PVC, 16 mg of oNPOE, and 2.2 mg of TDDATFAB in 1.0 mL of THF. Specifically, a 30 μ L aliquot of the THF solution was dropped from a 50 μ L syringe onto the gold disk rotating at 1500 rpm in a spin-coating device (model SCS-G3-8, Cookson Electronics, Providence, RI). The modified gold disk was removed from the spin coater and dried in air for at least 20 min.

2.2.3 Electrochemical Measurement

An electrochemical workstation (CHI 900A or CHI 600A, CH Instruments) was used for voltammetric measurement. A Pt wire counter electrode was employed in the following three-electrode cells:



The concentrations of each oxoanion are given in the Results and Discussion. The current carried by an anion from the aqueous phase to the membrane was defined to be negative. All electrochemical experiments were performed at 22 ± 3 °C.

Noticeably, additional setups and procedures were used for different voltammetric measurements. A piece of Teflon tube⁶ was put on a PVC/POT-modified gold electrode for cyclic voltammetry to define a disk-shaped membrane/water interface with a diameter of 1.5 mm. A PVC/POT-modified gold electrode was rotated during stripping voltammetry by using a modulated speed rotator (Pine Research Instrumentation). For stripping voltammetry of picomolar PFOS⁻, the electrochemical cell and rotator were placed in an Ar-filled polyethylene glove bag (AtmosBag, Aldrich), which was protected from airborne contaminants inside a class 100 vertical laminar flow hood (model AC632LFC, AirClean Systems, Raleigh, NC).¹² Inside the bag, Milli-Q water was collected and sample solutions were prepared. An as-prepared electrode was contaminated during preparation and was cleaned in the background Milli-Q water solution of supporting electrolytes (cell 2) by repeating stripping voltammetric measurements until no contaminant response was detected.

2.3 RESULTS AND DISCUSSION

2.3.1 Cyclic Voltammetry of Perfluoroalkanesulfonates

The transfer of perfluoroalkanesulfonates across the interface between water and the oNPOE/PVC membrane was studied by cyclic voltammetry to demonstrate their high lipophilicity in comparison with their alkanesulfonate counterparts. Specifically, PFOS⁻, perfluorohexanesulfonate (PFHS⁻), and perfluorobutanesulfonate (PFBS⁻) were studied as the perfluoroalkanesulfonates monitored by the U.S. EPA²⁶ and were compared with octanesulfonate (OS⁻). Their voltammograms were observed at different potentials in the order PFOS⁻ < PFHS⁻ <

PFBS⁻ < OS⁻ (Figure 2), where the potentials were calibrated against the formal potential of ClO₄⁻.¹² This order corresponds to the reversed order of lipophilicity, thereby confirming that a perfluoroalkanesulfonate with a longer chain is more lipophilic. In addition, a comparison of PFOS⁻ with OS⁻ indicates that a perfluoroalkanesulfonate is much more lipophilic than the alkanesulfonate with the same chain length. This result is ascribed to the electron-withdrawing effect of a perfluoroalkyl group, which reduces the electron density of the adjacent sulfonate group to be more weakly hydrated.³⁰ By contrast, the shapes of the cyclic voltammograms (CVs) for the different sulfonates were very similar. A peak-shaped wave on anodic potential sweep showed a diffusional tail, which corresponds to the planar diffusion of a sulfonate from the bulk aqueous solution to the membrane/water interface. A diffusional tail was not seen for the reverse wave, where the current quickly dropped to zero because the sulfonate was exhaustively stripped from the thin membrane into the aqueous phase. In addition, the background-subtracted CVs were integrated to ensure that charges due to transferred sulfonates return to nearly zero at the end of a potential cycle (data not shown). This exhaustive stripping is advantageous for the ultrasensitive voltammetric detection of picomolar PFOS⁻ (see below).

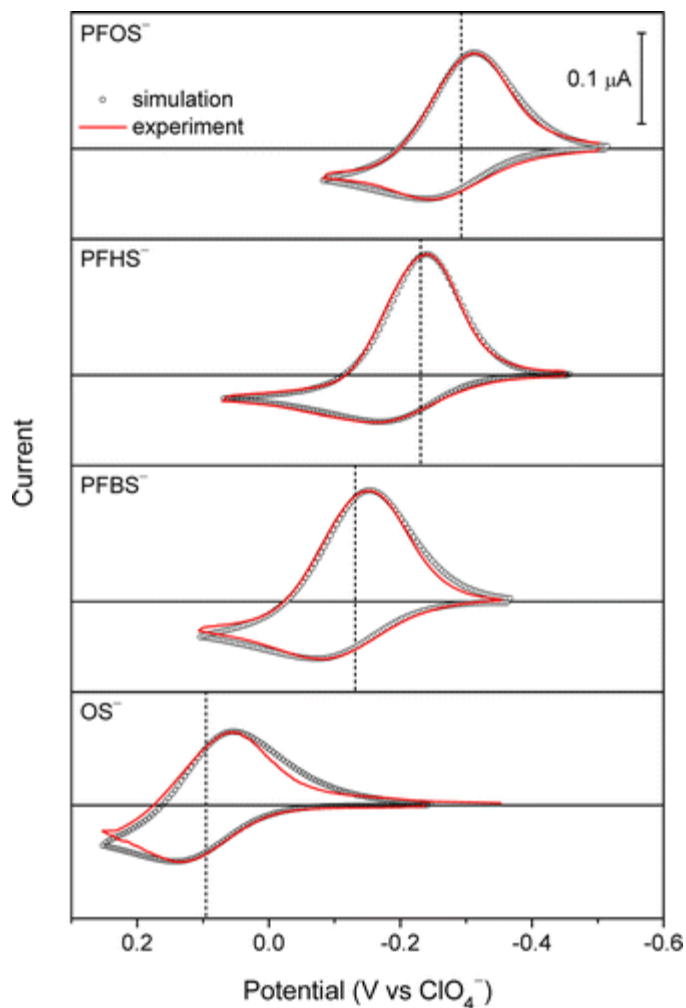


Figure 2. Background-subtracted CVs (red lines) of 20 μM perfluorooctanesulfonate, perfluorohexanesulfonate, perfluorobutanesulfonate, and octanesulfonate (from the top) in cell 1. The potential was applied to the gold electrode, swept at 0.1 V/s, and defined against the formal potential of perchlorate. Circles represent the CVs simulated by using the parameters listed in Table S-1 (Supporting Information). Dotted lines correspond to the formal potentials of the sulfonates.

The experimental CVs were analyzed quantitatively to determine formal ion-transfer potentials, which are related to formal partition coefficients as a measure of ion lipophilicity (eq. 1). Finite element analysis was required to simulate ion diffusion in the thin-layer membrane.⁴ Good fits were obtained for all experimental CVs with the CVs simulated for the reversible transfer of the sulfonates, which is fast and controlled by their diffusion. A characteristically high reverse peak current was fitted by considering a membrane thickness of $\sim 1 \mu\text{m}$ (Table S-1, Supporting Information), which is thin enough for the exhaustive stripping of membranous sulfonates. Noticeably, the good fits of the experimental CVs with the simulated CVs required the correction of the potential at the gold electrode because the applied potential polarized not only the PVC membrane/water interface but also the PVC/POT/gold junction for voltammetric ion-to-electron transduction.⁶ Empirically, the phase boundary potential at the PVC membrane/water interface, $\Delta w_m\phi$, is related to the applied potential, E , as given by⁴ (see the Supporting Information)

$$\Delta_w^m\phi - \Delta_w^m\phi_{\text{ClO}_4^-}^{0'} = (E - E_{\text{ClO}_4^-}^{0'}) \frac{\partial \Delta_w^m\phi}{\partial E} \quad (2)$$

where the applied potential was calibrated against the formal potential of ClO_4^- transfer so that $\Delta w_m\phi = \Delta w_m\phi_{\text{ClO}_4^-}^{0'}$ when $E = E_{\text{ClO}_4^-}^{0'}$.¹² The best fits were obtained by assuming that 60–69% of a change in the applied potential was used to change the phase boundary potential across the membrane/water interface, i.e., $\partial \Delta w_m\phi / \partial E = 0.60\text{--}0.69$ (Table S-1, Supporting Information), thereby broadening the resultant CVs and also enhancing their electrochemical reversibility.

2.3.2 Lipophilicity of Perfluoroalkanesulfonates: Fragmental Analysis

The formal potentials of perfluoroalkane- and alkanesulfonates were quantitatively compared by employing fragmental analysis³² to demonstrate that the 104 times higher lipophilicity of perfluoroalkanesulfonates is exclusively ascribed to the higher lipophilicity of their sulfonate groups. Specifically, the formal potential of a sulfonate, i , against that of perchlorate, $\Delta w_m \phi_i^{0'} - \Delta w_m \phi_{\text{ClO}_4}^{0'}$, was obtained by using eq. 2 with the parameters determined from the numerical analysis of CVs for perfluoroalkane- and alkanesulfonates (for the CVs of decane and dodecanesulfonates, DS^- and DDS^- , respectively, see Figure 7, Supporting Information). Figure 3 shows plots of $\Delta w_m \phi_i^{0'} - \Delta w_m \phi_{\text{ClO}_4}^{0'}$ values against the number of carbon atoms of the sulfonates, n , for the oNPOE/PVC membrane. Good linear relationships were obtained for the perfluoroalkane- and alkanesulfonates to yield

$$\Delta w_m \phi_i^{0'} - \Delta w_m \phi_{\text{ClO}_4}^{0'} = (n - 1)f(\text{CX}_2) + f(\text{CX}_3) + f(\text{SO}_3^-) \quad (3)$$

where f is a fragmental contribution of each unit and $X = \text{H}$ or F . Similar $f(\text{CF}_2)$ and $f(\text{CH}_2)$ values of -0.029 and -0.027 V, respectively, were obtained as slopes, thereby indicating that the lipophilicity of a CF_2 group is similar to that of a CH_2 group. By contrast, remarkably different $f(\text{CX}_3) + f(\text{SO}_3^-)$ values of 0.00 and 0.24 V were determined for perfluoroalkane- and alkanesulfonates, respectively, from eq 3 with $n = 1$. This difference of 0.24 V in $\Delta w_m \phi_i^{0'} - \Delta w_m \phi_{\text{ClO}_4}^{0'}$ values corresponds to a difference in $\text{Pi}^{0'}$ values of 4 orders of magnitude in eq 1. The 104 times higher lipophilicity of perfluoroalkanesulfonates is ascribed to a difference in $f(\text{SO}_3^-)$ values because similar $f(\text{CF}_3)$ and $f(\text{CH}_3)$ values are expected from similar $f(\text{CF}_2)$ and $f(\text{CH}_2)$ values.

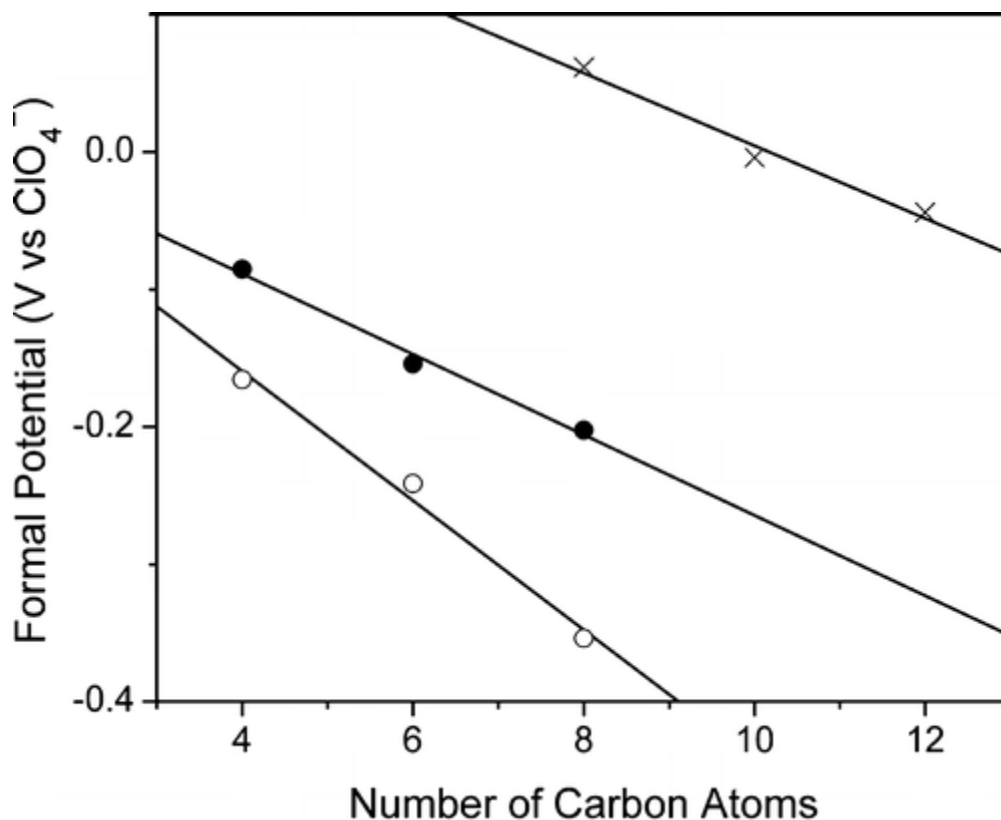


Figure 3. Formal potentials versus the number of carbon atoms of perfluoroalkanesulfonates (closed circles) and alkanesulfonates (crosses) for the oNPOE/PVC membrane. The formal potentials of the perfluoroalkanesulfonates for the fluorous membrane (open circles) were calculated from selectivity coefficients against perchlorate³⁶ by using eq. 4. Solid lines are the best fits with eq. 3.

The 10^4 -fold different lipophilicities of the sulfonate groups adjacent to perfluoroalkyl and alkyl groups are related to the solvation energies of the sulfonate groups not only in water but also in the oNPOE/PVC membrane. On one hand, the inductive effect of a perfluoroalkyl group on the electron density of the adjacent sulfonate group raises its hydration energy to enhance its lipophilicity. On the other hand, a lack of a specific interaction of a sulfonate group with oNPOE and PVC results in a relatively small change in the resultant solvation energy of the sulfonate group upon perfluorination. Overall, the difference in the hydration energies of the sulfonate groups

dominates the difference in their lipophilicities for the oNPOE/PVC membrane. Noticeably, this is not the case for 1-octanol, which can form a hydrogen bond with the oxygen atom of a sulfonate group. The sulfonate group adjacent to the perfluoroalkyl group is less charged and is a weaker hydrogen-bonding acceptor owing to the electron-withdrawing effect to be less favorably solvated in 1-octanol. Subsequently, PFOS⁻ is only 7.1×10 times more lipophilic than OS⁻ in 1-octanol.³⁰ By contrast, the $f(\text{CF}_2)$ and $f(\text{CH}_2)$ values with the oNPOE/PVC membrane are relatively similar to those of -0.036 V with 1-octanol.³⁰

2.3.3 Lipophilicity and Fluorophilicity of Perfluoroalkanesulfonates

We employed fragmental analysis to find that the lipophilicity of perfluoroalkanesulfonates is lower than their fluorophilicity. The fluorophilicity was evaluated by using the potentiometric selectivity coefficient determined by Bühlmann and co-workers.^{36, 37} With this potentiometric approach, a perfluoroalkanesulfonate was selectively partitioned between the aqueous phase and the fluorous membrane to obtain a Nernstian response based on a change in the phase boundary potential. Logarithmic potentiometric selectivity coefficients for PFOS⁻, PFHS⁻, and PFBS⁻ against perchlorate, $\log K_{i,\text{ClO}_4^{\text{pot}}}$, were -6.0 , -4.1 , and -2.8 , respectively, when perfluorooligoether, α -(heptafluoropropyl)- ω -(pentafluoroethoxy)-poly[oxy(1,1,2,2,3,3-hexafluoro-1,3-propanediyl)], was used as the fluorous membrane doped with a fluorous anion exchanger.³⁶ We converted the selectivity coefficients to differences between formal potentials as given by³⁹

$$\Delta_w^m \phi_i^{0'} - \Delta_w^m \phi_{\text{ClO}_4}^{0'} = -\frac{2.303RT}{z_i F} \log K_{i,\text{ClO}_4}^{\text{pot}} \quad (4)$$

The resultant $\Delta w_m \phi_{i0'} - \Delta w_m \phi_{ClO_4 0'}$ values were used as a measure of fluorophilicity to yield a linear relationship against the number of carbon atoms as expected from eq. 3 (Figure 3). Importantly, the fluorophilicity of a perfluoroalkanesulfonate is higher than its lipophilicity for the o-NPOE/PVC membrane. More quantitatively, fragmental analysis with eq. 3 reveals that this difference originates from a difference in $f(CF_2)$ values of -0.047 and -0.029 V for the fluorous and o-NPOE/PVC membranes, respectively. This result indicates that a CF_2 group is more favorably solvated in the fluorophilic membrane than in the lipophilic oNPOE/PVC membrane. By contrast, both membranes gave an identical $f(CF_3) + f(SO_3^-)$ value of -0.029 V. The $f(CF_3)$ value for the fluorous membrane should be more negative than that for the oNPOE/PVC membrane as expected from the more negative $f(CF_2)$ value for the fluorous membrane. Therefore, the $f(SO_3^-)$ value for the oNPOE/PVC membrane is more negative, thereby indicating that a sulfonate group is more stabilized in the oNPOE/PVC membrane although the sulfonate group would be strongly ion-paired with an anion exchanger in the fluorous membrane.⁴⁰

2.3.4 Stripping Voltammetry of PFOS⁻

The remarkably high lipophilicity of PFOS⁻ is highly advantageous for its ultrasensitive detection by stripping voltammetry because a more lipophilic ion can be preconcentrated at a higher concentration in the thin double-polymer membrane on the gold electrode to yield a lower detection limit.⁷ In fact, this study shows that PFOS⁻ is the most lipophilic among the perfluoroalkanesulfonates and perfluoroalkancarboxylates monitored by the U.S. EPA²⁶ (see below for the lipophilicity of the carboxylates). In the preconcentration step, an aqueous analyte ion is potentiostatically transferred into the confined volume of the solid-supported membrane,

which is eventually saturated with the analyte ion.⁴ The resultant equilibrium concentration of the analyte ion in the membrane, c_m , is given by the Nernst equation as

$$Y = \frac{c_m}{c_w} = \exp\left[-\frac{z_r F(\Delta_w^m \phi_p - \Delta_w^m \phi_1^{0'})}{RT}\right] \quad (5)$$

where Y is a preconcentration factor, c_w is the bulk aqueous concentration of the analyte ion, and $\Delta_w^m \phi_p$ is the phase boundary potential during preconcentration. Equation 5 predicts that, with a given $\Delta_w^m \phi_p$ value, the preconcentration factor is higher for a more lipophilic anion with a more negative $\Delta_w^m \phi_1^{0'}$ value.

We performed stripping voltammetry of 10 nM PFOS⁻ at preconcentration times of 0.5–40 min (Figure 4A) to determine a high preconcentration factor, Y , of 2.2×10^5 . The electrode was rotated at 2000 rpm to achieve steady states, which facilitate data analysis. The voltammetric peak grew at a longer preconcentration time, which increased the concentration of PFOS⁻ in the membrane. More quantitatively, the stripping voltammogram was integrated to obtain the charge, $Q(t_p)$, at the preconcentration time t_p . This total charge is a sum of the charge due to the stripping of PFOS⁻ preconcentrated in the membrane and the charge due to background processes during the stripping step, Q_{bg} , which is mainly charging of the membrane/water interface. In theory, $Q(t_p)$ is given by⁴

$$Q(t_p) = Q_{eq} \left[1 - \exp\left(-\frac{i_l t_p}{Q_{eq}}\right) \right] + Q_{bg} \quad (6)$$

where Q_{eq} is the equilibrium charge due to the exhaustive stripping of PFOS⁻ from a saturated membrane and i_l is the limiting current during the preconcentration step under the rotating-electrode condition. The best fit of eq 6 with the experimental plot (Figure 4B) gives $i_l = 1.7$ nA, $Q_{eq} = 4.1$ μ C, and $Q_{bg} = 1.7$ μ C. This limiting current is immeasurably small by cyclic voltammetry and is given by the Levich equation as⁴¹

$$i_1 = 0.62z_iFA D_w^{2/3} \omega^{1/2} \nu^{-1/6} c_w \quad (7)$$

where D_w is the diffusion coefficient of a target ion in the aqueous phase, ω is the rotation speed, and ν is the viscosity of the aqueous electrolyte solution. Equation 7 with $A = 0.196 \text{ cm}^2$, $D_w = 5.7 \times 10^{-6} \text{ cm}^2/\text{s}$ (Table S-1, Supporting Information), and $\nu = 0.010 \text{ cm}^2/\text{s}$ gives $c_w = 10.8 \text{ nM}$, which agrees with the spiked PFOS⁻ concentration of 10 nM. In addition, the preconcentration factor, Y , can be calculated from the Q_{eq} value as given by⁴

$$Q_{\text{eq}} = z_i F Y V_m c_w \quad (8)$$

where V_m is the membrane volume. A Y value of 2.2×10^5 is obtained from the Q_{eq} value by using eq. 8 with $V_m = 2.0 \times 10^{-8} \text{ L}$ for a 1 μm thick and 5 mm diameter membrane. This large preconcentration factor corresponds to a large overpotential, $\Delta w_m \phi_p - \Delta w_m \phi_{\text{PFOS}0'}$, of 0.32 V in eq 5. This large overpotential can be applied without the limitation of the potential window because of the high lipophilicity of PFOS⁻, i.e., very negative $\Delta w_m \phi_{\text{PFOS}0'}$.

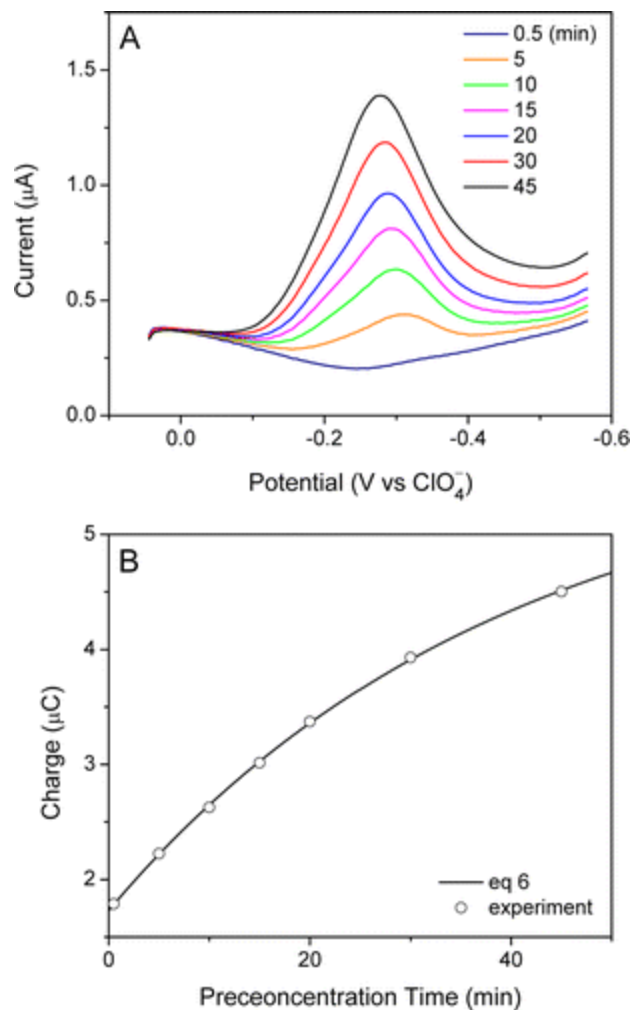


Figure 4. (A) Stripping voltammograms of 10 nM PFOS⁻ (cell 2) at different pre-concentration times. The potential was applied to the gold electrode, swept at 0.1 V/s, and defined against the formal potential of perchlorate. (B) Charge during stripping voltammetry (circles) and best fit with eq. 6 (solid line).

2.3.5 Picomolar Detection Limit for PFOS⁻

Stripping voltammetric responses to PFOS⁻ were measured after 30 min of preconcentration to yield a detection limit of 50 pM (Figure 5A). The electrode was rotated at 2000 rpm to enhance the mass transport of PFOS⁻ from water to the membrane/water interface. The background-subtracted stripping voltammograms (Figure 8, Supporting Information) show the clearer peak currents that linearly vary with the PFOS⁻ concentration in a range of 0–1 nM (Figure 5B). Remarkably, the detection limit of 50 pM (0.025 µg/L) for PFOS⁻ is much lower than that of 0.86 nM by potentiometry with the fluoros membrane³⁶ and is lower than the minimum reporting level of 0.04 µg/L in drinking water set by the U.S. EPA.²⁶ Moreover, the slope of the calibration plot was assessed quantitatively to find its consistency with theory. A peak current response, i_p , based on the exhaustive and reversible transfer of an analyte ion from a thin double-polymer membrane is given by⁴²

$$i_p = \frac{z_i^2 F^2 v V_m c_m(t_p)}{4RT} \quad (9)$$

with

$$Y(t_p) = \frac{c_m(t_p)}{c_w} = Y \left[1 - \exp\left(-\frac{i_l}{Q_{eq}} t_p\right) \right] \quad (10)$$

where v is the potential sweep rate during the stripping process, $c_m(t_p)$ and $Y(t_p)$ are the membrane ion concentration and preconcentration factor at the preconcentration time of t_p , and i_l/Q_{eq} is independent of c_w (see eqs. 7 and 8) and is given by the aforementioned i_l and Q_{eq} values. Noticeably, the potential sweep rate in eq. 9 corresponds to a change in the phase boundary potential across the membrane/water interface, which is slower than the actual potential sweep rate of 0.1 V/s by a factor of $\partial\Delta w_m\phi/\partial E$ (~ 0.65 ; Table S-1, Supporting Information).

Subsequently, eq 9 gives a slope of 1.26×10^2 A/M for a plot of i_p versus c_w for PFOS^- . This slope is close to a value of $(1.01 \pm 0.08) \times 10^2$ A/M as determined from three calibration plots including the plot in Figure 5B.

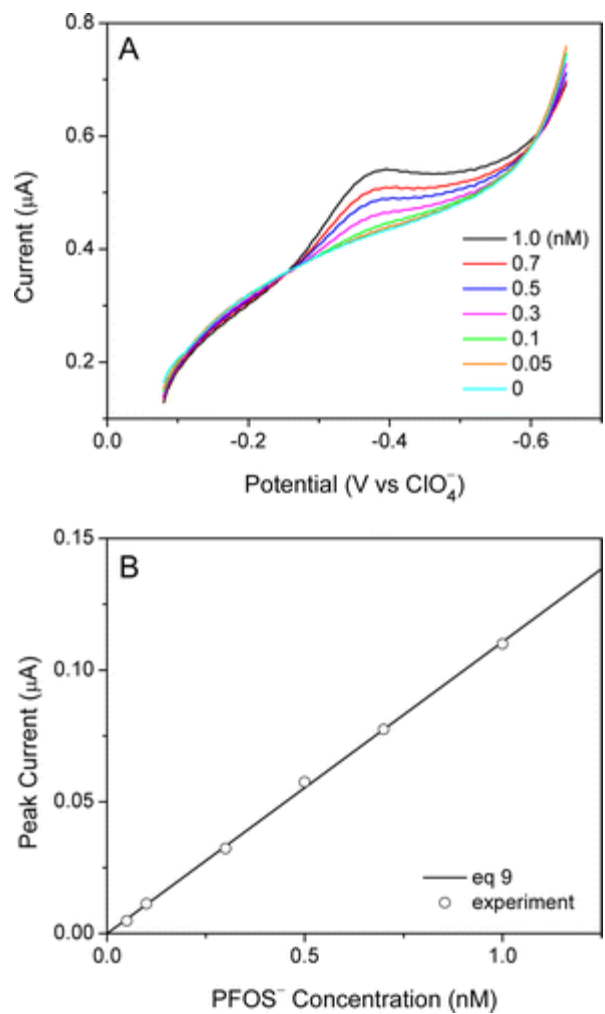


Figure 5. (A) Stripping voltammograms of 0–1 nM PFOS⁻ (cell 2) after 30 min of preconcentration. The potential was applied to the gold electrode, swept at 0.1 V/s, and defined against the formal potential of perchlorate. (B) Background-subtracted peak current versus PFOS⁻ concentration (circles) and best fit with eq. 9 (solid line).

Importantly, the contamination of background electrolyte solutions with a lipophilic anion had to be prevented to enable the detection of picomolar PFOS⁻ by stripping voltammetry. The peak potential of the contaminant anion was more positive than that of PFOS⁻ only by ~0.1 V (Figure 9, Supporting Information), thereby indicating the relatively high lipophilicity of the contaminant anion. Moreover, the contaminant responses were much higher than the responses to 0.1–1 nM PFOS⁻, which were seriously distorted. The contaminant responses are not due to the transfer of a cation from the membrane to water because these responses were not seen when extra care was taken to protect the sample solutions from airborne contaminants (Figure 5A). Specifically, the electrochemical cell was placed in the Ar-filled polyethylene glove bag, which was accommodated in the class 100 vertical laminar flow hood as reported elsewhere.^{1, 12} In addition, we extensively cleaned the PVC/POT-modified electrodes, which were seriously contaminated during their preparation. A contaminant response was readily detected by stripping voltammetry upon the first immersion of a newly prepared electrode in the background aqueous solution. Eventually, no contaminant response was detectable (Figure 5A) after the electrode was washed in two background solutions during stripping voltammetry with 5 min of preconcentration.

2.3.6 Cyclic Voltammetry of Perfluoroalkancarboxylates

The transfer of perfluoroalkancarboxylates at the oNPOE/PVC membrane was studied by cyclic voltammetry (Figure 6) to demonstrate their low lipophilicity and high oxidizability in comparison with those of perfluoroalkanesulfonates. Initially, we investigated PFO⁻, perfluorohexanoate (PFH⁻), and perfluorobutanoate (PFB⁻), which have the same number of carbon atoms as the perfluoroalkanesulfonates studied in this work (see above). A perfluoroalkancarboxylate with a longer chain is expected to be more lipophilic and was indeed transferred at less positive potentials,

thereby yielding the order of lipophilicity as $\text{PFO}^- > \text{PFH}^- > \text{PFB}^-$. These perfluoroalkancarboxylates, however, are much less lipophilic than the perfluoroalkanesulfonates with the same number of carbon atoms, which possess much less positive formal potentials (dotted lines in Figure 6). Remarkably, PFOS^- is even more lipophilic than perfluorodecanoate (PFD^-) and perfluorododecanoate (PFDD^-) (Figure 9, Supporting Information). This result indicates that PFOS^- is more lipophilic than any perfluoroalkancarboxylate monitored by the U.S. EPA (i.e., PFO^- , perfluoroheptanoate, and perfluorononanoate).²⁶ The lower lipophilicity of perfluoroalkancarboxylates is due to the intrinsically stronger hydration of the carboxylate group,⁴³ which is smaller and more basic than the sulfonate group. Nevertheless, the least lipophilic perfluoroalkancarboxylate, PFB^- , is as lipophilic as tetradecanoate (TD^-) as shown in Figure 6, where both carboxylates were transferred at similar potentials. The similar lipophilicities are due to the inductive effect of the perfluoroalkyl group on reducing the electron density of the adjacent carboxylate group. Noticeably, a lack of reverse peak for TD^- is due to its oxidative consumption at the POT-modified gold electrode as discussed in the following paragraph.

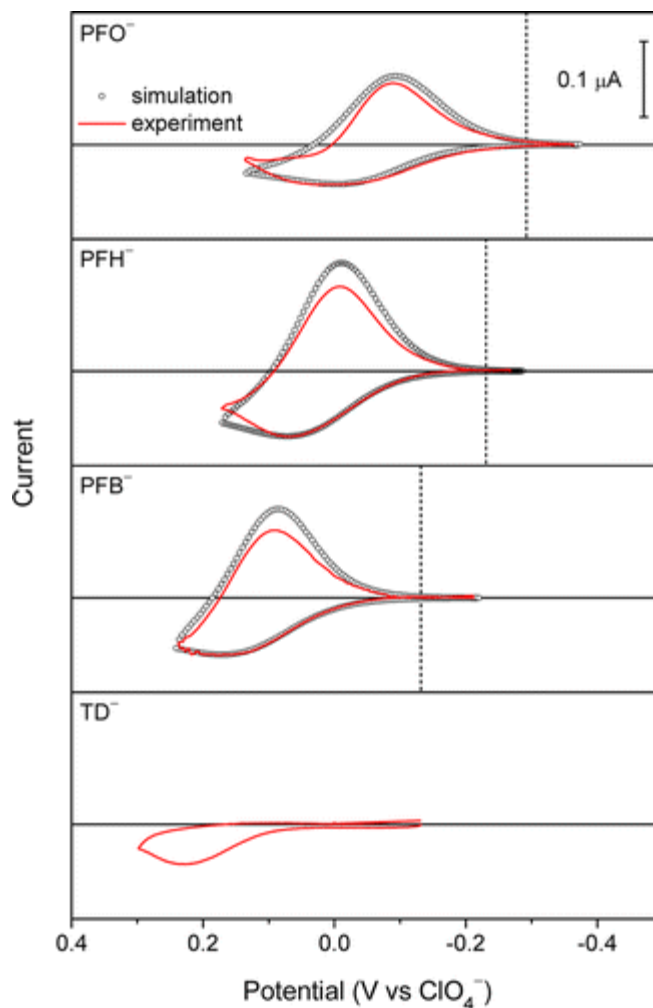


Figure 6. Background-subtracted CVs (red lines) of 20 μM perfluorooctanoate, perfluorohexanoate, and perfluorobutanoate and 10 μM tetradecanoate (from the top) in cell 1. The potential was applied to the gold electrode, swept at 0.1 V/s, and defined against the formal potential of perchlorate. Circles represent the CVs simulated by using the parameters listed in Table S-1 (Supporting Information). Dotted lines correspond to the formal potentials of the sulfonates with the same number of carbon atoms.

Unfortunately, the lipophilicity of the perfluoroalkancarboxylates cannot be determined quantitatively owing to their oxidative loss at the POT-modified gold electrode, which is seen as the lower cathodic peaks of the experimental CVs than those of the simulated CVs (Figure 6). Accordingly, the charge during experimental cyclic voltammetry does not return to zero upon the completion of a potential cycle (data not shown), although the reverse peak does not have a diffusional tail. This result confirms that the perfluoroalkancarboxylates are not exhaustively stripped from the membrane during the reverse potential sweep. We propose that the loss of the perfluoroalkancarboxylates in the oNPOE/PVC membrane is due to their oxidative decarboxylation based on the Kolbe reaction⁴⁴ at the POT-modified gold electrode as given by



This reaction not only consumes the carboxylates but also does not generate any anionic product, thereby decreasing the cathodic response during the reverse potential sweep. We confirmed the oxidation of PFO⁻ at the PVC/POT/gold junction by cyclic voltammetry with the nonpolarizable PVC/water interface (see Figure 11, Supporting Information). Moreover, a reverse peak was not seen for TD⁻ (Figure 6), which is more readily oxidizable. The lower oxidizability of perfluoroalkancarboxylates is ascribed to the inductive effect and is supported further by the fact that similarly positive potentials were applied to the gold electrode for PFB⁻ and TD⁻ to observe a reverse peak only for the former. Noticeably, the oxidation of perfluoroalkancarboxylates will be preventable by employing a conducting polymer film that is oxidized at less positive potentials than the POT film for voltammetric ion-to-electron transduction.

2.3.7 Voltammetry versus Potentiometry with the oNPOE/PVC Membrane

Interestingly, this study revealed that the voltammetric responses based on the interfacial transfer of PFOS⁻ and PFO⁻ can be obtained by using the oNPOE/PVC membrane, which gave no potentiometric response to either species.³⁷ This voltammetric result strongly suggests that no potentiometric response of the oNPOE/PVC membrane to highly lipophilic PFO⁻ and PFOS⁻ is due to the insufficient solubility of these fluorophilic anions in the lipophilic membrane doped with 5% (w/w) tridodecylmethylammonium chloride. Detrimentally, all chloride ions must be replaced with PFO⁻ or PFOS⁻, i.e., conditioning,³⁶ to obtain a Nernstian potentiometric response to the analyte ion. Advantageously, ion-transfer voltammetry needs no conditioning and requires a much lower PFOS⁻ concentration of <2.2 mM ($=c_m$ from eq. 5 with $Y = 2.2 \times 10^5$ and $c_w = 10$ nM) in the membrane even when the highest current response of $\sim 1.5 \mu\text{A}$ in this study is obtained (Figure 4A). On the other hand, no extraction of PFDD⁻ into the oNPOE/PVC membrane was observed voltammetrically (Figure 10, Supporting Information), thereby indicating that this extremely fluorophilic anion was not detectably soluble in the lipophilic membrane. Importantly, the CV of PFDD⁻ showed its interfacial adsorption, which would not be detectable by potentiometry. This result exemplifies the power of voltammetry in diagnostic strength to understand the ion-transfer mechanism.³ In fact, adsorption was also observed for PFO⁻ (around 0.1 V in Figure 6), while both extraction and adsorption were observed for PFD⁻ (Figure 10, Supporting Information) in addition to DS⁻ and DDS⁻ (Figure 7, Supporting Information). As expected,⁴⁵ the adsorption peak currents were proportional to the potential sweep rates (data not shown).

2.4 CONCLUSIONS

In this work, we demonstrated the ultrasensitive voltammetric detection of highly lipophilic perfluoroalkyl oxoanions at a picomolar level by using a thin oNPOE/PVC membrane supported by a POT-modified gold electrode. Specifically, ion-transfer stripping voltammetry enabled the detection of down to 50 pM PFOS⁻, which is the most lipophilic among the six perfluoroalkyl oxoanions monitored by the U.S. EPA.⁽¹⁴⁾ This detection limit is lower than the minimum reporting level of PFOS⁻ in drinking water set by the U.S. EPA²⁶ and is the lowest achieved electrochemically for any perfluoroalkyl oxoanion so far.^{25, 36} The high lipophilicity of PFOS⁻ contributed not only to the unprecedentedly low detection limit but also to its highly selective detection in the presence of 1 mM aqueous electrolytes.

This work also indicates that the fluorous membrane^{36, 37} is highly attractive for the ultrasensitive voltammetry of the multiple perfluoroalkyl oxoanions monitored by the U.S. EPA²⁶ because of the high fluorophilicity of a perfluoroalkyl group in comparison to its lipophilicity as discovered in this study. Our theory (eq. 5) predicts that stripping voltammetry with the fluorous membrane will give a lower detection limit for a perfluoroalkyl oxoanion, which can be potentiostatically accumulated at a higher concentration in the fluorous membrane. Moreover, the multiple perfluoroalkyl oxoanions will be simultaneously detectable by using the single voltammetric electrode based on the fluorous membrane owing to larger differences in formal potentials among the oxoanions with different chain lengths. On the other hand, the high resistivity of the fluorous membrane due to the strong ion pairing of supporting electrolytes⁴⁰ must be lowered for its voltammetric applications to avoid a significant ohmic potential drop across the membrane.

2.5 SUPPORTING INFO

2.5.1 Cyclic Voltammetry of Alkyl Sulfonates

Dodecyl and decyl sulfonates (DDS^- and DS^- , respectively) were studied by CV (Figure 7) to determine their formal potentials. The extraction of the sulfonates into the membrane gave the first anodic wave, which was paired with the larger cathodic peak based on their exhaustive stripping. The numerical analysis of the extraction waves, however, was complicated by a pair of the surface waves based on the adsorption of the sulfonates at the oNPOE/PVC membrane as observed around 0.15 V. Therefore, a formal potential was estimated from a reverse peak potential by assuming that their difference is identical to that of OS^- (Figure 2).

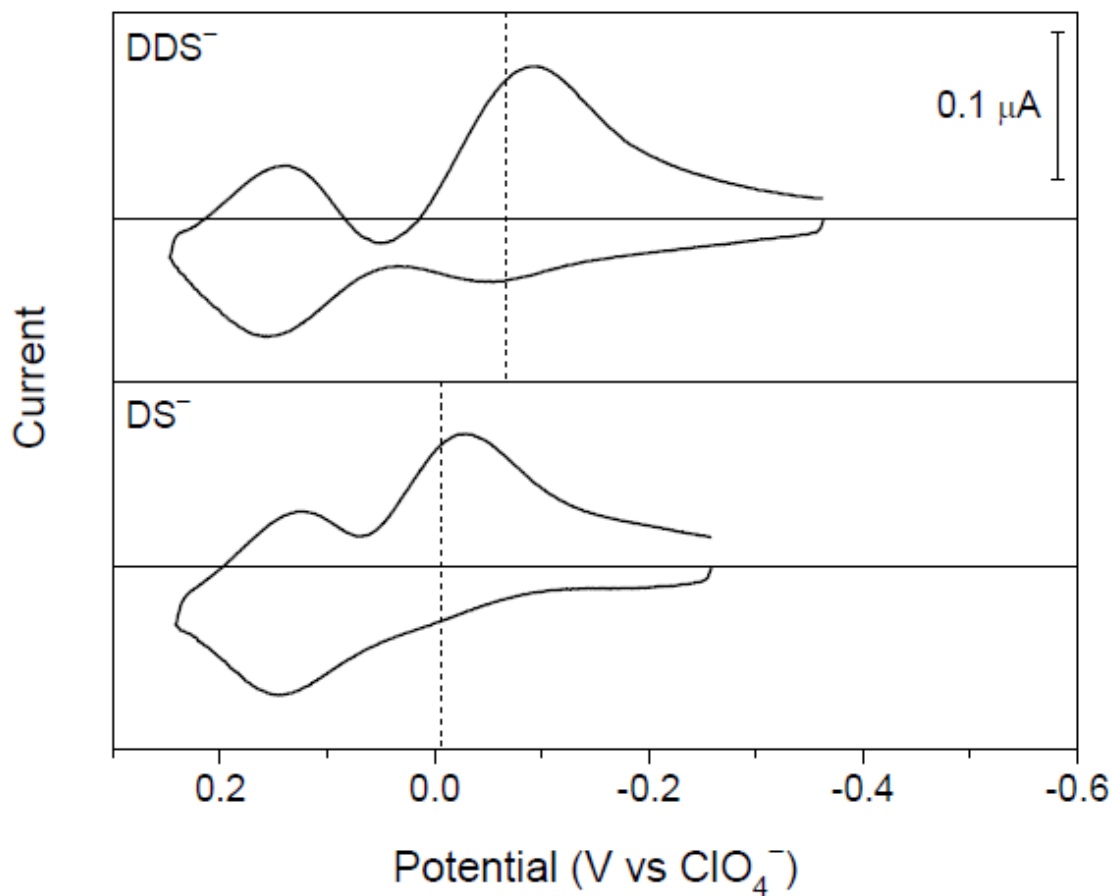


Figure 7. Background-subtracted CVs (red lines) of 20 μM dodecyl and decyl sulfonates (from the top) in cell 1. The potential was applied to the gold electrode, swept at 0.1 V/s, and defined against the formal potential of perchlorate. Dotted lines correspond to the formal potentials of the sulfonates.

2.5.2 Background-Subtracted Stripping Voltammograms of Picomolar PFOS⁻

Peak-shaped responses to 0.05–1 nM PFOS⁻ were more clearly seen after background subtraction (Figure 8). The peak currents of the background-subtracted stripping voltammograms were linear to the PFOS⁻ concentrations (Figure 5B).

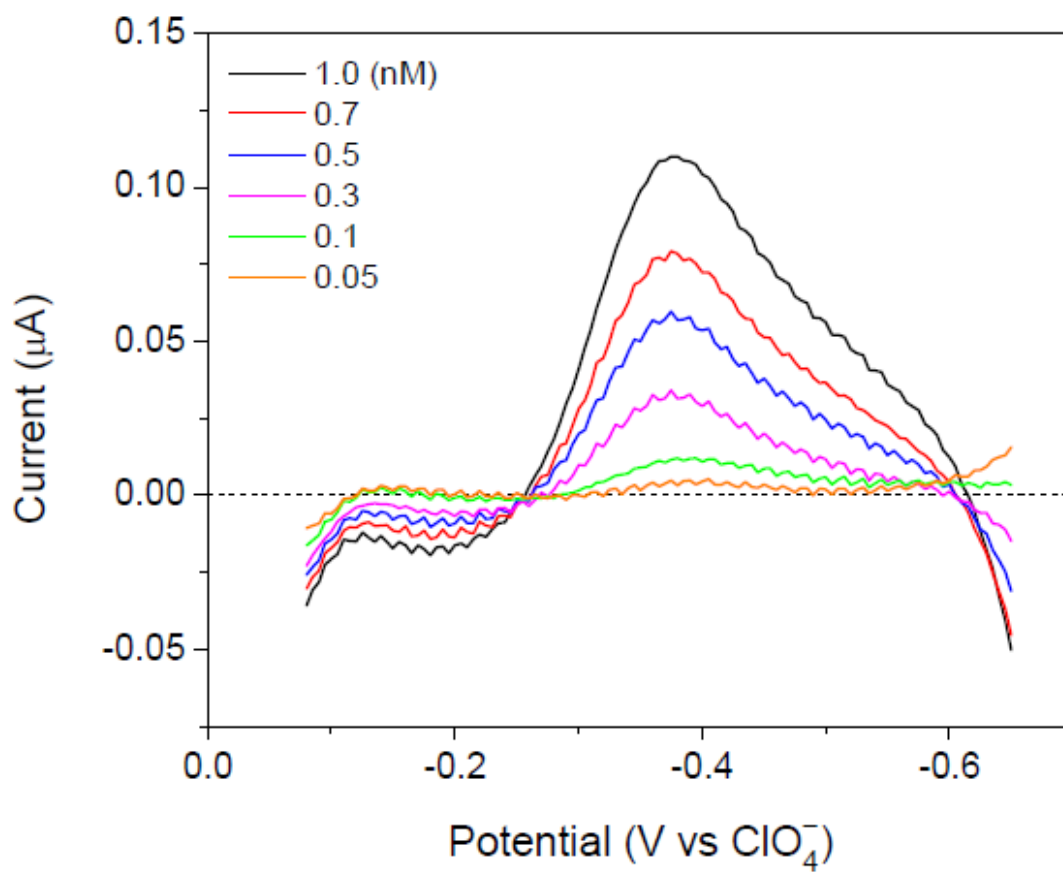


Figure 8. Background-subtracted stripping voltammograms of 0.05–1 nM PFOS⁻ (cell 2) after 30 min preconcentration. The potential was applied to the gold electrode, swept at 0.1 V/s, and defined against the formal potential of perchlorate. The dotted line represents zero current.

2.5.3 Stripping Voltammetric Responses to a Contaminant Anion

Significant stripping voltammetric responses to a contaminant anion were observed near PFOS⁻ responses (Figure 9) when the electrochemical cell (cell 2) was exposed to air during the measurements. The contaminant responses were not seen when the electrochemical cell was placed in the Ar-filled bag (Figure 5A) and the electrode was sufficiently cleaned.

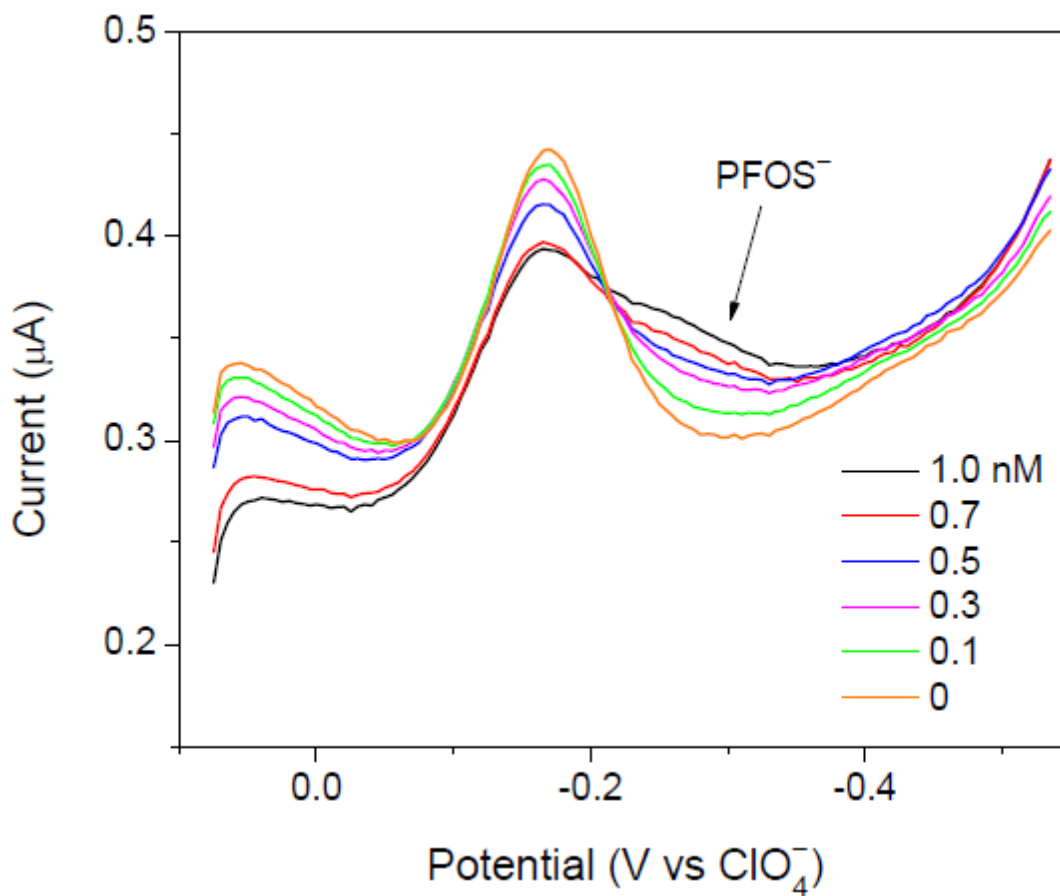


Figure 9. Stripping voltammograms of 0–1 nM PFOS⁻ (cell 2) after 30 min preconcentration in the presence of a contaminant anion in the sample solutions. The potential was applied to the gold electrode, swept at 0.1 V/s, and defined against the formal potential of perchlorate.

2.5.4 Lipophilicity of Perfluoroalkyl Carboxylates

The interfacial behaviors of perfluorododecanoate (PFDD^-) and perfluorodecanoate (PFD^-) were studied by CV to compare their lipophilicity with the lipophilicity of PFOS^- (Figure 10). All peak potentials of PFDD^- and PFD^- are more positive than the formal potential of PFOS^- (dotted line), which is more lipophilic. Interestingly, PFDD^- gave two pairs of surface waves based on adsorption and desorption at the membrane/water interface, thereby indicating that PFDD^- cannot be extracted into the oNPOE/PVC membrane. By contrast, the extraction of PFD^- into the membrane gave the anodic wave paired with the much higher cathodic wave based on exhaustive stripping while a pair of surface waves was observed around 0.05 V.

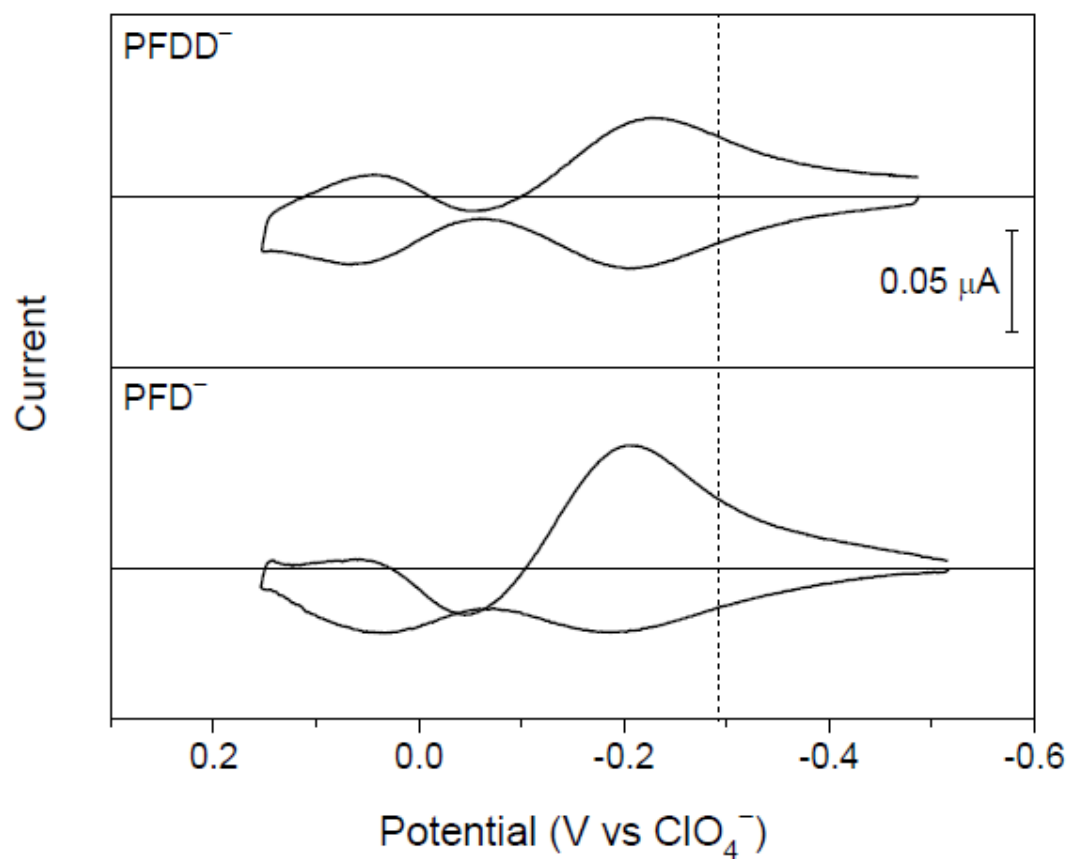


Figure 10. Background-subtracted CVs (red lines) of 20 μM perfluorododecanoate and perfluorodecanoate (from the top) in cell 1. The potential was applied to the gold electrode, swept at 0.1V/s, and defined against the formal potential of perchlorate. The dotted line corresponds to the formal potential of PFOS⁻.

2.5.5 Oxidation of PFO⁻ at the PVC/POT/Gold Junction

We employed non-polarizable PVC/water interfaces⁶ to voltammetrically study the oxidation of PFO⁻ at the PVC/POT/gold junction. In this experiment, a oNPOE/PVC/POT-modified electrode was immersed in the solution of 8 mM tetrabutylammonium (TBA⁺) perchlorate, which is partitioned into the PVC membrane to fix the phase boundary potential across the membrane/water interface as given by⁴⁶

$$\Delta_w^m \phi = \frac{\Delta_w^m \phi_{\text{PFO}}^{0'} + \Delta_w^m \phi_{\text{TBA}}^{0'}}{2} \quad (\text{S-2})$$

By contrast, the PVC/POT/gold junction can be polarizable externally to yield a CV controlled by the oxidation and reduction of the POT film (black line Figure 11). This well-defined CV resembles that of the POT film in acetonitrile.⁶ By contrast, a distorted CV (red line) was obtained when 1 mM TBA⁺ and PFO⁻ were added to the TBAClO₄ solution as chloride and sodium salts, respectively, to partition TBAPFO into the PVC membrane. The distorted CV indicates the oxidation of PFO⁻ at the PVC/POT/gold junction.

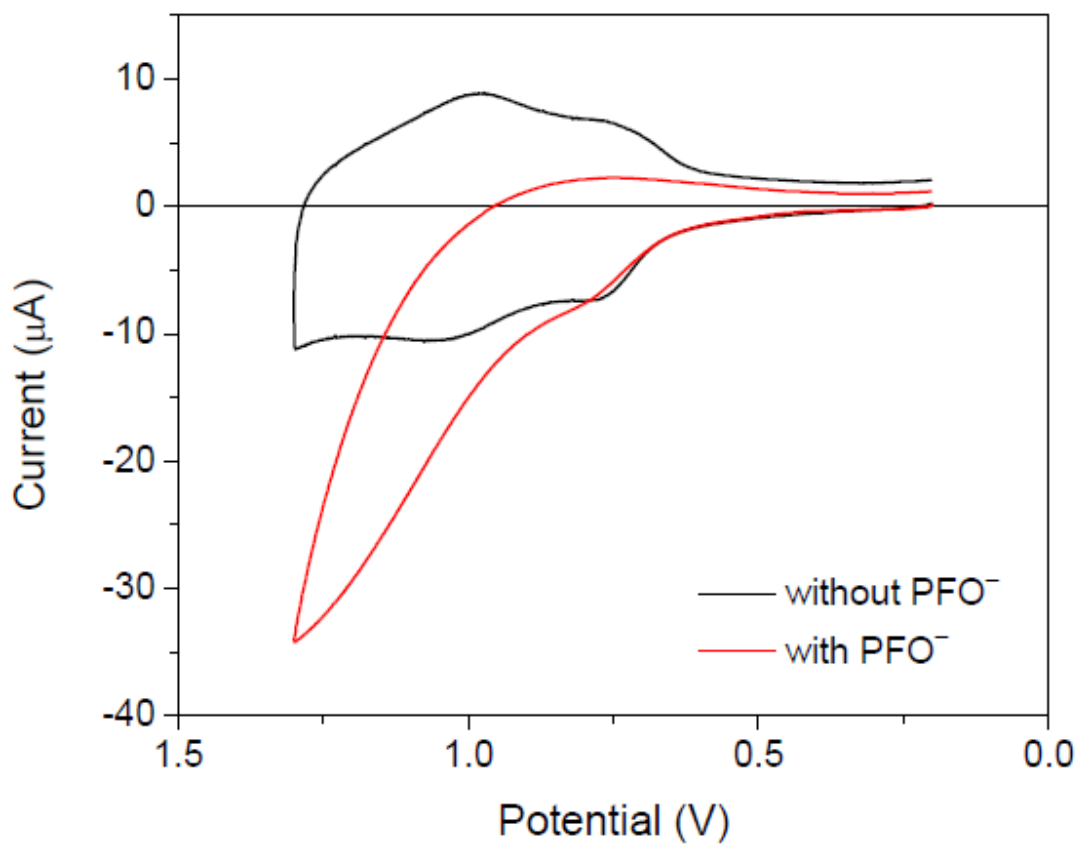


Figure 11. CVs of a POT film with a PVC membrane/water interface non-polarized by partitioning of TBAClO₄. The potential was applied to the gold electrode against a Ag/AgCl reference electrode in 3 M KCl. Potential sweep rate, 0.1 V/s.

3.0 DEVELOPMENT OF NEW CONDUCTING POLYMER:

POLY(4,4'-DIBUTOXY-2,2'-BITHIOPHENE)

3.1 BACKGROUND

Carrying on from the surfactant project we desired to look at new conducting polymers to determine if there is one suitable for carboxylate detection where POT had failed due to the hypothesized oxidation of the carboxylate surfactants and also the inconsistent surfactant peak potentials. To this end a conducting polymer that lies between POT and PEDOT in terms of redox potential was sought. A suitable choice was hypothesized to be poly(4,4'-dibutoxy-2,2'-bithiophene) for its intermediate polarity of having only one oxygen atom compared to the two oxygen atoms in the monomeric unit of PEDOT and the absence of oxygen atoms in POT.⁴⁷ Long chains of this polymer, however, have proven difficult in making from single monomer units as polymerization will usually stop at short chain species.^{52, 48} One way around this problem is to start the polymerization process from the dimer instead (Figure 12), which can lead to much longer polymer species.⁵²

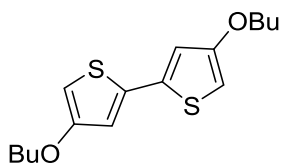


Figure 12. Proposed new conducting polymer in its dimer form: 4,4'-dibutoxy-2,2'-bithiophene

The higher redox stability of the new conducting polymer in both oxidized and reduced states may provide a more reproducible and stable potential for voltammetric measurements, thereby eliminating the need of potential calibration by using a reference ion such as perchlorate. Ultimately with a good conducting polymer for carboxylate surfactants we could then move to study other environmentally and biologically significant ions and accordingly modify our electrode system as necessary in order to improve upon the current detection limits of those ions using ion-transfer voltammetry. For instance, past attempts at sensitive detection of Ag^+ and Pb^{2+} were hindered by reduction of the cations by the conducting polymer (PEDOT), while detection of thiocyanate has also revealed that the anion undergoes oxidation from POT. Thus this proposed intermediate conducting polymer could be useful for both cations and anions.

3.2 SYNTHESIS OF 4,4'-DIBUTOXY-2,2'-BITHIOPHENE

A synthesis for the dimer species 4,4'-dibutoxy-2,2'-bithiophene was undertaken via CuO/KI catalyzed n-butoxylation of 4,4'-dibromo-2,2'-bithiophene using sodium n-butoxide (Figure 13).⁴⁹

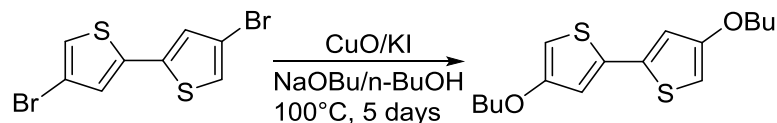


Figure 13. Synthesis of 4,4'-dibutoxy-2,2'-bithiophene from 4,4'-dibromo-2,2'-bithiophene

We hypothesize that the reaction proceeds through a halogen exchange type mechanism catalyzed by CuI generated in situ from CuO and KI.⁵⁰ The resultant more electrophilic iodothiophene can

then be readily attacked by the nucleophilic n-butoxide species. A side product of the reaction observed during this synthesis was the single-butoxylated dimer species 4-bromo-4'-butoxy-2,2'-bithiophene which may indicate that the reaction proceeds through step-wise replacement of the bromine atoms (Figure 14). Furthermore, initial trials of this reaction showed lower yields of the dibutoxy dimer product relative to the monobutoxy product.

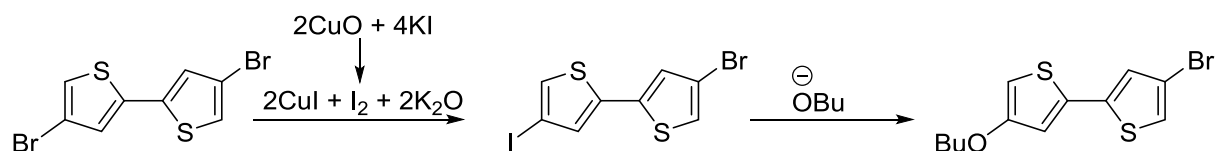


Figure 14. Hypothesized step-wise halogen exchange and butoxylation of 4,4'-dibromo-2,2'-bithiophene leading to the monobutoxy side product 4-bromo-4'-butoxy-2,2'-bithiophene

The unreacted starting dibromo dimer accounted for a significant portion of the missing yield in the early trials as well. The fact that not all of the starting material was converted and that more of the monobutoxy dimer compound was made than the dibutoxy dimer was believed to be caused by slow halogen exchange on the thiophene ring from possibly aged potassium iodide.

In detail, three separate trials of the synthesis were performed. In the first trial both the yield of the dibutoxy dimer product (~10%) and the conversion of the starting material (~20%) were poor. It was initially suspected that the sodium used was too old and may have been too contaminated with sodium oxide preventing adequate formation of sodium butoxide. A second trial was performed with freshly purchased sodium which still gave a similarly low yield (~8%), but this time with a better conversion of the starting material (~40%) observed by a higher yield of the monobutoxy side product.

It was next thought that the poor yield may be stemming from slow halogen exchange due to issues with the potassium iodide or copper oxide catalysts. Specifically, we were worried that the potassium iodide used up to that point may have been too old, and because of its hygroscopic nature possibly inflated in weight due to absorbed moisture or decomposed due to reaction with water.⁵¹ Furthermore, it was hypothesized that the overall reaction could be accelerated by using a smaller particle size of copper oxide providing a larger surface area for the catalytic reaction to occur.

To this end, a third trial of the synthesis was undertaken with new potassium iodide and smaller copper oxide particles (10 μ m vs. 50 μ m). Additionally the recovered dibromo starting material and monobutoxy dimer from the first two syntheses were used as starting reagents instead of new 4,4'-dibromo-2,2'-bithiophene. The starting reaction mixture for the third trial consisted of ~45% dibromo starting material and ~55% monobutoxy dimer. The results of the third trial showed an improved yield of the dibutoxy dimer product (~30%) as well as an improved conversion of the dibromo compound (~75%). Under the hypothesis that the reaction proceeds stepwise from the dibromo dimer to the monobutoxy dimer and finally to the dibutoxy dimer, the higher yield makes sense in terms of the fact that roughly half of the dibromo compound was already transformed into the monobutoxy dimer compound. However, while the conversion is quite improved, the yield is still low relative to that reported in the literature and may still be indicative of an overall slow reaction.⁴⁹

Aside from the reaction proceeding slowly, another possible explanation for the low yield of the dibutoxy product may be from loss of the product due to acid induced polymerization, possibly during the silica gel chromatography. While the silica gel used was prepared with 2% triethylamine to deactivate its acidic properties, it is not known for certain if the volume of the triethylamine

solution was enough to completely deactivate the silica gel. This was suspected due to varying colors observed for the dibutoxy product. Darker shades of the product from yellow to brown to black were thought to be from higher concentration of polymerization products. It may be the case that the shorter chain polymers are able to co-elute off the silica gel column with the dibutoxy dimer causing the darker color changes, while the longer chain polymers stick onto the column and in effect reduce the recovered yield. In this regard, in the first two syntheses a lesser volume of the 2% triethylamine solution was used to deactivate the silica gel and the resultant color of the dibutoxy product was in fact darker than in the third synthesis where a larger volume of the 2% triethylamine solution was used.

The general procedure for the three synthetic trials was carried out as follows:⁴⁹ Sodium metal (0.40 g, 17.40 mmoles) was completely dissolved in *n*-butanol (25mL). To the resulting solution, copper oxide (0.25 g, 3.14 mmoles), potassium iodide (0.04 g, 0.24 mmoles) and 4,4'-dibromo-2,2'-bithiophene (1.00 g, 3.09 mmoles) were added and the mixture was then stirred at 100°C for 3 days. Following this, more potassium iodide (0.04 g, 0.24 mmoles) was added and the reaction was resumed at 100°C for 2 more days. Afterwards, the reaction was stopped and filtered, and then added into water. The organic layer was extracted with ether, subsequently washed with water and then dried with magnesium sulfate. The crude mixture was completely evaporated and then purified by column chromatography using hexanes as the eluent. The silica gel (particle size 40-63µm) used for chromatography was initially neutralized by mixing it with a solution of 2% triethylamine in hexanes. The purified product appeared as yellow crystals; ¹H NMR (CDCl₃): δ 0.98 (t, 6H), 1.50 (m, 4H), 1.76 (m, 4H), 3.94 (t, 4H), 6.11 (d, 2H), 6.82 ppm (d, 2H).

3.3 ELECTROCHEMICAL POLYMERIZATION

Upon completion of the synthesis, electropolymerization of the purified dibutoxy dimer product was tested. While previous polymerizations of this dimer have been performed by chemical means, no electrochemical polymerization of the dimer has been reported previously. Successful polymerization of the dimer into a sufficiently long polymer chain is proven through deposition onto a gold electrode. This is true because in contrast to shorter polymer chains, long polymer chains become insoluble in the acetonitrile solvent used for electrochemical polymerization to the point that they come out of solution and form a deposited layer onto the gold electrode.

For electrochemical polymerization, the dimer was dissolved into acetonitrile at a concentration of 0.01M along with a supporting organic electrolyte salt (TDDA-TFAB, C = 0.03M). The acetonitrile solution was added to a carbon cell which was used as the counter electrode in a cyclic voltammetry three-electrode setup with a Au working electrode (5mm diameter) and platinum wire as the reference electrode. Electropolymerization of the dibutoxy dimer (Figure 15) was performed by sweeping the potential towards positive potentials until an anodic current of -0.60mA was observed. Afterwards the potential was cycled back to reduce the newly formed polymer. At this point, two new pair of peaks were observed in the cyclic voltammogram. The process was repeated three-four times in order to generate a polymer of suitable length, with each repeated cycle increasing the magnitude of the peak currents. The potential cycles were stopped at the negative potential side of the cyclic voltammogram leaving the polymer in a reduced state which showed a strong purplish-blue color.

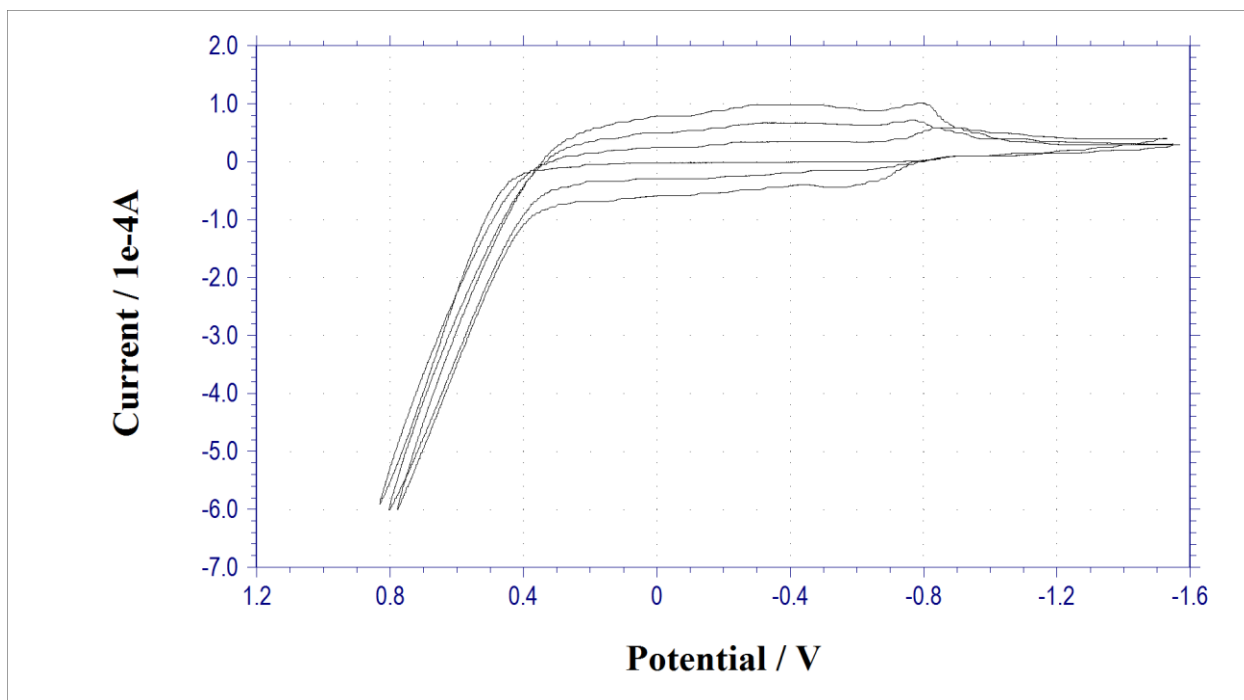


Figure 15. Electropolymerization of 4,4'-bitoxy-2,2'-bithiophene in acetonitrile ($C = 0.01\text{M}$) with TDDA-TFAB ($C = 0.03\text{M}$); Scan rate = 0.1V/s , Au working electrode, Pt wire reference electrode, carbon graphite cell as counter electrode. The potential was cycled three times and ended at the negative side of the potential window.

Further characterization was done on the modified electrode by rinsing it in acetonitrile for 1min and then performing a CV (Figure 16) of the polymer in a monomer-free acetonitrile solution solely containing the TDDA-TFAB supporting organic electrolyte salt ($C = 0.03\text{M}$). The CV was measured by cycling the potential three times between the cathodic and anodic peaks of the polymer. In this case, the potential was halted at the positive side in order to leave the polymer in its oxidized state which was transparent in appearance. The more defined shape of the CV peaks in the monomer free experiment relative to that in the initial electropolymerization CV could be due to dissolution of the smaller chain length polymers during the acetonitrile wash as well as during the time the electrode stayed in the acetonitrile solutions during the electrochemical

experiments. Overall the CV shape of poly(4,4'-dibutoxy-2,2'-bithiophene) seemed to agree with what had been previously reported in the literature for the same polymer generated by means of chemical rather than electrochemical polymerization.⁵²

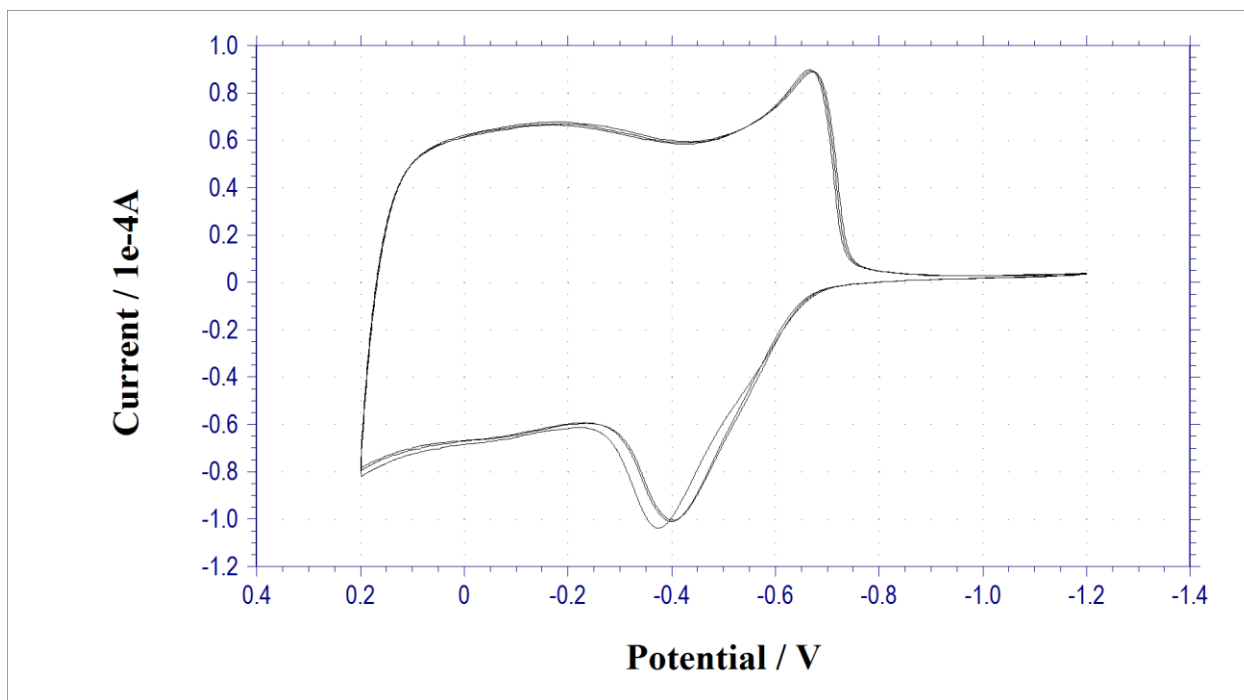


Figure 16. Monomer free CV of poly(4,4'-bitoxy-2,2'-bithiophene) in acetonitrile with TDDA-TFAB ($C = 0.03\text{M}$); Scan rate = 0.1V/s , Au working electrode, Pt wire reference electrode, carbon graphite cell as counter electrode. The potential was cycled three times starting at the negative side of the potential window and ending at the positive side.

In contrast to the monomer free CVs of PEDOT- C_{10} , poly(4,4'-dibutoxy-2,2'-bithiophene) showed much sharper cathodic and anodic peaks. Additionally the new polymer showed a prominent single pair of peaks whereas PEDOT- C_{10} shows two cathodic peaks that are virtually equivalent in terms of peak current, and a minor shoulder peak coming off from the broad anodic peak. However, the single pair of peaks in poly(4,4'-dibutoxy-2,2'-bithiophene) was accompanied by a much smaller pair of peaks occurring at a more positive potential and appearing as broad

humps. Due to the similarity of the electropolymerization conditions for PEDOT-C₁₀ and poly(4,4'-dibutoxy-2,2'-bithiophene), a comparison could also be made of the magnitude of the peak currents for the two different polymers generated from identical potential cycles. Specifically, separate comparisons of the polymers for both three cycle and four cycle electropolymerization showed that PEDOT-C₁₀ gave a higher anodic peak current, while poly(4,4'-dibutoxy-2,2'-bithiophene) gave a higher cathodic peak current.

4.0 CONCLUSIONS

Ion transfer voltammetry has been previously performed on various types of ions using ion-selective electrodes. Highlighted here is the work done on surfactant ions, where the high lipophilicities of these ions allowed for higher preconcentration into the organic PVC membrane during stripping voltammetry and subsequently a lower detection limit. The lipophilic trends of different types of surfactants were found and measured by their calibrated standard potential during cyclic voltammetry. Of the four different groups of surfactants studied, the alkyl carboxylates showed issues of incomplete charge replacement during their CVs due to oxidation of those ions by the conducting polymer POT. Meanwhile, previous issues observed for the other conducting polymer PEDOT were also hoped to be fixed, which included reduction of certain cations during ion-transfer voltammetry and lack of redox stability in the reduced state of the polymer. To this end, a new conducting polymer poly(4,4'-dbutoxy-2,2'-bithiophene) was synthesized and tested by electrochemical polymerization. The success of initial electropolymerization trials opens up the possibility of testing this new conducting polymer further in the double polymer setup with PVC and on the ions that were oxidized and reduced by POT and PEDOT respectively.

BIBLIOGRAPHY

- ¹ Kabagambe, B., Izadyar, A., Amemiya, S. *Anal. Chem.* **2012**, *84*, 7979.
- ² Chen, L. D., Bühlmann, P., Ion-Selective Electrodes with Ionophore-Doped Sensing Membranes. In *Supramolecular Chemistry: From Molecules to Nanomaterials*; Gale, P.A. and Steed, J.W., Ed.; Wiley: 2012; p. 2539.
- ³ Ishimatsu, R., Izadyar, A., Kabagambe, B., Kim, Y., Kim, J., Amemiya, S. *J. Am. Chem. Soc.* **2011**, *133*, 16300.
- ⁴ Kim, Y., Amemiya, S. *Anal. Chem.* **2008**, *80*, 6056.
- ⁵ Richardson, S. D., Ternes, T. A. *Anal. Chem.* **2014**, *86* (6), 2813.
- ⁶ Guo, J., Amemiya, S. *Anal. Chem.* **2006**, *78*, 6893.
- ⁷ Kim, Y., Rodgers, P. J., Ishimatsu, R., Amemiya, S. *Anal. Chem.* **2009**, *81*, 7262.
- ⁸ Heinze, J., Frontana-Uribe, B. A., Ludwigs, S. *Chem. Rev.* **2010**, *110*, 4724.
- ⁹ Bobacka, J. *Electroanalysis.* **2006**, *18* (1), 7.
- ¹⁰ Sankaran, B., Reynolds, J.R. *Macromolecules* **1997**, *30*, 2582.
- ¹¹ Garada, M. B., Kabagambe, B., Kim, Y., Amemiya, S. *Anal. Chem.* **2014**.
- ¹² Kabagambe, B., Garada, M. B., Ishimatsu, R., Amemiya, S. *Anal. Chem.* **2014**, *86*, 7939.
- ¹³ Houde, M.; De Silva, A. O.; Muir, D. C. G.; Letcher, R. J. *Environ. Sci. Technol.* **2011**, *45*, 7962.
- ¹⁴ Vecitis, C. D.; Park, H.; Cheng, J.; Mader, B. T.; Hoffmann, M. R. *Front. Environ. Sci. Eng. China* **2009**, *3*, 129.
- ¹⁵ Zareitalabad, P.; Siemens, J.; Hamer, M.; Amelung, W. *Chemosphere* **2013**, *91*, 725.

- ¹⁶ Chang, E. T.; Adami, H. O.; Boffetta, P.; Cole, P.; Starr, T. B.; Mandel, J. S. *Crit. Rev. Toxicol.* **2014**, *44*, 1.
- ¹⁷ Carter, K. E.; Farrell, J. *Environ. Sci. Technol.* **2008**, *42*, 6111.
- ¹⁸ Ochiai, T.; Iizuka, Y.; Nakata, K.; Murakami, T.; Tryk, D. A.; Fujishima, A.; Koide, Y.; Morito, Y. *Diamond Relat. Mater.* **2011**, *20*, 64.
- ¹⁹ Xiao, H.; Lv, B.; Zhao, G.; Wang, Y.; Li, M.; Li, D. *J. Phys. Chem. A.* **2011**, *115*, 13836.
- ²⁰ Zhuo, Q. F.; Deng, S.; Yang, B.; Huang, J.; Wang, B.; Zhang, T.; Yu, G. *Electrochim. Acta.* **2012**, *77*, 17.
- ²¹ Zhuo, Q.; Deng, S.; Yang, B.; Huang, J.; Yu, G. *Environ. Sci. Technol.* **2011**, *45*, 2973.
- ²² Niu, J.; Lin, H.; Xu, J.; Wu, H.; Li, Y. *Environ. Sci. Technol.* **2012**, *46*, 10191.
- ²³ Niu, J.; Lin, H.; Gong, C.; Sun, X. *Environ. Sci. Technol.* **2013**, *47*, 14341.
- ²⁴ Manivel, A.; Velayutham, D.; Noel, M. *Ionics* **2010**, *16*, 153.
- ²⁵ Zhang, T.; Zhao, H.; Lei, A.; Quan, X. *Electrochemistry* **2014**, *82*, 94.
- ²⁶ Methods and Contaminants for the Unregulated Contaminant Monitoring Rule 3 (UCMR 3). UCMR 3 Contaminants and Corresponding Analytical Methods. Assessment Monitoring (List 1 Contaminants). <http://water.epa.gov/lawsregs/rulesregs/sdwa/ucmr/ucmr3/methods.cfm#assessment> (accessed October 2014).
- ²⁷ Shoemaker, J. A.; Grimmett, P. E.; Boutin, B. K. *Method 537. Determination of Selected Perfluorinated Alkyl Acids in Drinking Water by Solid Phase Extraction and Liquid Chromatography/Tandem Mass Spectrometry (LC/MS/MS)*, version 1.1; EPA/600/R-08/092; U.S. Environmental Protection Agency: Cincinnati, OH, 2009.
- ²⁸ Arrigan, D. W. M.; Herzog, G.; Scanlon, M. D.; Strutwolf, J. Bioanalytical Applications of Electrochemistry at Liquid-Liquid Micro-Interfaces. In *Electroanalytical Chemistry*; Bard, A. J., Zoski, C. G., Eds.; Taylor & Francis: Boca Raton, FL, 2013; Vol. 25, p 105.
- ²⁹ Amemiya, S.; Wang, Y.; Mirkin, M. V. Nanoelectrochemistry at the Liquid/Liquid Interfaces. In *Specialist Periodical Reports in Electrochemistry*; Compton, R. G., Wadhawan, J. D., Eds.; Royal Society of Chemistry: Cambridge, U.K., 2013; Vol. 12, p 1.
- ³⁰ Jing, P.; Rodgers, P. J.; Amemiya, S. *J. Am. Chem. Soc.* **2009**, *131*, 2290.
- ³¹ Kelly, B. C.; Ikonomou, M. G.; Blair, J. D.; Morin, A. E.; Gobas, F. *Science* **2007**, *317*, 236.

- ³² Sangster, J. Octanol–Water Partition Coefficients: Fundamentals and Physical Chemistry; John Wiley & Sons: New York, 1997; Vol. 2.
- ³³ Reymond, F.; Steyaert, G.; Carrupt, P. A.; Testa, B.; Girault, H. H. *J. Am. Chem. Soc.* **1996**, *118*, 11951.
- ³⁴ Rodgers, P. J.; Amemiya, S. *Anal. Chem.* **2007**, *79*, 9276.
- ³⁵ Amemiya, S.; Kim, J.; Izadyar, A.; Kabagambe, B.; Shen, M.; Ishimatsu, R. *Electrochim. Acta* **2013**, *110*, 836.
- ³⁶ Chen, L. D.; Lai, C.-Z.; Granda, L. P.; Fierke, M. A.; Mandal, D.; Stein, A.; Gladysz, J. A.; Bühlmann, P. *Anal. Chem.* **2013**, *85*, 7471.
- ³⁷ Boswell, P. G.; Anfang, A. C.; Bühlmann, P. *J. Fluorine Chem.* **2008**, *129*, 961.
- ³⁸ Izadyar, A.; Kim, Y.; Ward, M. M.; Amemiya, S. *J. Chem. Educ.* **2012**, *89*, 1323.
- ³⁹ Amemiya, S. Potentiometric Ion-Selective Electrodes. In *Handbook of Electrochemistry*; Zoski, C. G., Ed.; Elsevier: New York, 2007; p 261.
- ⁴⁰ Boswell, P. G.; Buhlmann, P. *J. Am. Chem. Soc.* **2005**, *127*, 8958.
- ⁴¹ Bard, A. J.; Faulkner, L. R. *Electrochemical Methods: Fundamentals and Applications*, 2nd ed.; John Wiley & Sons: New York, 2001; p 339.
- ⁴² Bard, A. J.; Faulkner, L. R. *Electrochemical Methods: Fundamentals and Applications*, 2nd ed.; John Wiley & Sons: New York, 2001; p 455.
- ⁴³ Kihara, S.; Suzuki, M.; Sugiyama, M.; Matsui, M. *J. Electroanal. Chem.* **1988**, *249*, 109.
- ⁴⁴ Vijn, A. K.; Conway, B. E. *Chem. Rev.* **1967**, *67*, 623.
- ⁴⁵ Bard, A. J.; Faulkner, L. R. *Electrochemical Methods: Fundamentals and Applications*, 2nd ed.; John Wiley & Sons: New York, 2001; p 591.
- ⁴⁶ Samec, Z. *Pure Appl. Chem.* **2004**, *76*, 2147.
- ⁴⁷ Dietrich, M., Heinze, J. *Synthetic Metals.* **1991**, *41-43*, 503.
- ⁴⁸ Tschuncky, P., Heinze, J. *Synthetic Metals.* **1993**, *55-57*, 1603.
- ⁴⁹ Goldoni, F., Iarossi, D., Mucci, A., Schenetti, L. *J. Heterocyclic Chem.* **1997**, *34*, 1801.
- ⁵⁰ Sheppard, T. *Org. Biomol. Chem.*, **2009**, *7*, 1043.

⁵¹ Pahuja, D. N., Rajan, M. G., Borkar, A. V., Samuel, A. M. *Health Phys.* **1993**, 65 (5), 545.

⁵² Faid, K., Cloutier, R., Leclerc', M. *Macromolecules.* **1993**, 26, 2501.